All manuscripts are peer reviewed by experts in the respective field. Authors of the manuscripts bear responsibility for their content, credibility and reliability.
Editorial board doesn't expect the manuscripts' authors to always agree with its opinion.

European Journal of Molecular Biotechnology

2020

Is. 1

# C O N T E N T S

## Articles

**Articles**

**Quantum Mechanical Descriptors of Π-Conjugated Imidazolinone Compounds: A DFT Study**

Abdelkhalk Aboulouard [a], Ali Barhoumi [b], Abdellah Zeroual [b], Abdessamad Tounsi [c], Mohammed El idrissi [a],[*]

[a] Sultan Moulay Slimane University, Beni Mellal, Morocco
[b] Chouaïb Doukkali University, El Jadida, Morocco
[c] Research Team in Applied Chemistry and Modeling ERCAM, Beni-Mellal, Morocco

**Abstract**

In this work, natural bond orbital (NBO) analysis, nonlinear optical and the thermodynamic properties of six organic π-conjugated compounds based on imidazolinone have been analyzed by employing density functional theory (DFT) level employing B3LYB/6-31G (d, p) basis set. NBO analysis reveals that the intra-intermolecular charge transfer occurs within the molecules leading to the stabilization. The predicted nonlinear optical (NLO) properties like; polarizability and first hyperpolarizabiliy support showed that the six organic π-conjugated studied imidazolone derivatives compounds could attract the interests for future investigation. The LUMO energy is increasingly concentrated around the nitrogen group of the chain by the acceptor groups with the increase of their mesomeric attractor effect in the following order − P6 < P1 < P4 < P5 < P3 < P2-. This explains the decrease in gap energy ΔE(P2) > ΔE (P3)> ΔE (P5) > ΔE (P4) > ΔE(P1)> ΔE(P6).

**Keywords:** imidazolinone, DFT, B3LYB, NBO, NLO, nonlinear optical, polarizability, hyperpolarizabiliy.

**1. Introduction**

Over recent years, imidazolinones have gained much attention due to their environmentally friendly molecular properties. Imidazolinones have been used to study the solar cell activity (Sharma, Handique, 2016). Moreover, imidazolinones are well known for their optoelectronic, biological, pharmacological and photochemical properties (Chuang et al., 2009; Bhattacharjya et al., 2008; Bahadur, Srivastava, 2004; You et al., 2000). In this study, NLO analysis of the studied molecules were evaluated at the B3LYP basis set. The chemical descriptors such as the Polarizability (α), anisotropic (Δα), polarizability (β), hyperpolarizability <β> and isotropic β// were computed using the TD-DFT method. Furthermore, NBO analysis were examined with DFT/B3LYB, CAM-B3LYP, HSEH1PBE, HCTH407 and WB97XD basis set (Bahçeli et al., 2015).

The most used photovoltaic technology is silicon solar cell which is considered as inorganic ones (Kim et al., 2005). The disadvantages of silicon solar cells are their price and complicated fabrication procedures. Due to such disadvantages, a new generation of solar cells has been emerged. This includes organic solar cells (OSCs) (Yang et al., 2005; Park et al., 2009), perovskite

---

[*] Corresponding author
E-mail addresses: m.elidrissi2018@gmail.com (M. El idrissi)

solar cells (Green et al., 2009; Lee, 2007) dye sensitized solar cells (Hadipour, 2008; Ameri, 2009), quantum dots solar cells (Boreland, 2008; Lu et al., 2015).

## 2. Materials and methods

All geometry optimizations computation was executed using the Gaussian 09 programs (Frisch et al., 2009). The geometries of the products were fully optimized through DFT calculations using the B3LYP functional (Becke, 1993; Yang, 1988), jointly in addition to the 6-311G (d,p) basis set (Francl, 1982). Initial structures were cleaned repeatedly to obtain normalized geometry. Each of the P1 and P2 was then subjected for successive optimization using DFT methods in conjunction with appropriate basis sets. Final optimization of these molecules is achieved using DFT/B3LYP/6-311G (d, p) method. Final optimization of these molecules is achieved using DFT/B3LYP/6-311G (d, p) method. For computation of linear and NLO properties, the additional key of "optical" was included in the study. Following equations are used for the extraction of parameters and properties of these impurities. Molecular complexity is the criterion that can be related with Δα (Chen et al., 2017; Aihara et al., 1999; Obot et al., 2009; Ghanadzadeh et al., 2000). More the complexity of structure more is the anisotropy of polarizability (Δα) (Zhan et al., 2003; Xue et al., 2004).

While dipole moment (DM) is the measure of α of a molecule in its ground state, α is the intrinsic capacity of a molecule of having a dipole when it is assaulted with an external electric field (Harris et al., 1999; Lim et al., 1999). If a molecule is present in a weak, static electric field (of strength, F), then the total energy (E) of the molecule can be express as a Taylors series.

$$E_F = E_0 - \mu_\alpha F_\alpha - \frac{1}{2!}\alpha_{\alpha\beta}F_\alpha F_\beta - \frac{1}{3!}\alpha_{\alpha\beta\gamma}F_\alpha F_\beta F_\gamma - \frac{1}{3!}\alpha_{\alpha\beta\gamma\delta}F_\alpha F_\beta F_\gamma F_\gamma \ldots\ldots\ldots (1)$$

E0 denotes the energy of the molecule in the absence of an external electrical field. Energy ($E_0$), dipole moment ($\mu_\alpha$), polarizability ($\alpha_{\alpha\beta}$), and first- and second-order hyperpolarizability ($\beta_{\alpha\beta\gamma}$ and $\gamma_{\alpha\beta\gamma\delta}$, respectively) denote the molecular properties. First polarizability and second hyperpolarizabilities are expressed as tensor quantities, whereas subscripts single, double, etc., denote the first-rank and second-rank tensor, etc., in Cartesian coordinate (Desharnais et al., 2003).

If the external field lies on any one of the three orthogonal Cartesian axes, then the components of the induced moments will be parallel to the field. In that case, off-diagonal terms of the tensor, ααβ vanish. Under these conditions, the expected value of αand DM obtained as:

$$DM = \sqrt{(\mu_X^2 + \mu_Y^2 + \mu_Z^2)} \quad \text{Or} \quad <\alpha_{STATIC}> = \frac{(\alpha_{XX} + \alpha_{YY} + \alpha_{ZZ})}{3} \qquad (2)$$

In case of the anisotropic orientation of the external field, the anisotropy of the polarizability ($<\Delta\alpha>$) can be computed as:

$$<\Delta\alpha> = \left[\frac{(\alpha_{XX}-\alpha_{YY})^2 + (\alpha_{YY}-\alpha_{ZZ})^2 + (\alpha_{YY}-\alpha_{ZZ})^2 + 6(\alpha_{XX}^2 - \alpha_{XY}^2 + \alpha_{YZ}^2)^2}{2}\right]^{\frac{1}{2}} \qquad (3)$$

Similarly, the first-order ($\beta_{\alpha\beta\gamma}$) and second-order ($\gamma_{\alpha\beta\gamma\delta}$) hyperpolarizability is calculated from components of respective tensors that are obtained from the Gaussian 09 output file.

$$\begin{cases} <\alpha_{STATIC}> = (\beta_X^2 + \beta_Y^2 + \beta_{XZ}^2)^{\frac{1}{2}} \\ \beta_i = \beta_{iii} + \frac{1}{3}\sum_{i\neq k}(\beta_{ikk} + \beta_{kik} + \beta_{kki}) \\ <\alpha_{STATIC}> = \left[\sqrt{\begin{array}{c}(\beta_{XXX} + \beta_{XYY} + \beta_{XZZ})^2 + (\beta_{YYY} + \beta_{YZZ} + \beta_{YXX})^2 \\ + (\beta_{ZZZ} + \beta_{ZXX} + \beta_{ZYY})^2\end{array}}\right] \end{cases} \quad (4)$$

$$<\alpha_{STATIC}> = \frac{\gamma_{XXXX} + \gamma_{YYYY} + \gamma_{ZZZZ} + 2\gamma_{YYXX} + 2\gamma_{YYZZ} + 2\gamma_{ZZXX}}{5} \qquad (5)$$

All these optical terms have been calculated using appropriate basis set that contains polarized and diffused functions for high accuracy, in that DFT/B3LYP/6-311G (d, p) was preferred.
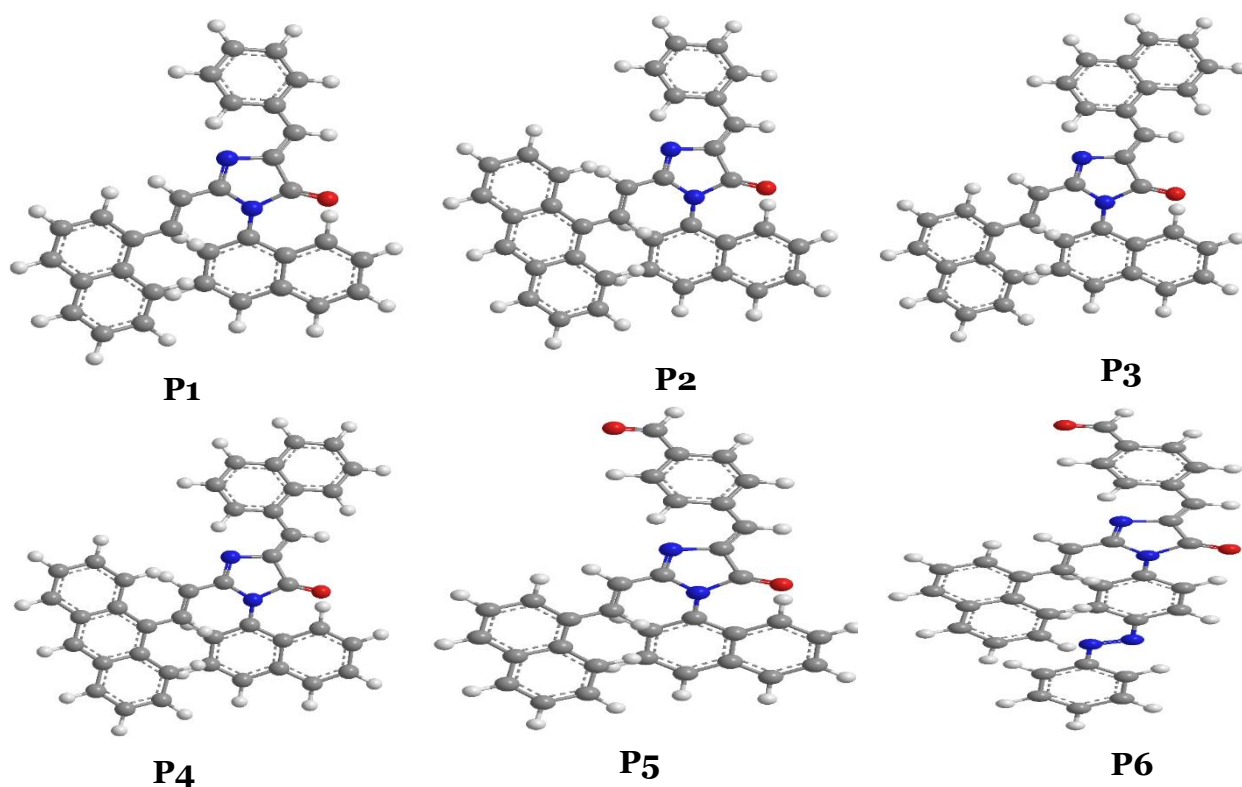
**Fig. 1.** Chemical structure of studied compounds

### 3. Results and discussion

The highest occupied molecular orbital (HOMO) and lowest unoccupied molecular orbital (LUMO) for P1 to P6 imidazolone derivatives are presented in (Figure 1), along with their optimized structures. While HOMO delocalizes over bonds of P1, and P2, it is less prominent for P1 to P6. Notably, the delocalization is uniform in P1. By the use of DFT/B3LYP/6-311G (d, p) level of theory, the extracted energies for HOMO, LUMO, and ΔE for P1 and P2 are presented in (Table 1) and compared in (Figure 2).

**Table 1.** HOMO, LUMO, and band gap energies for P1 to P6 imidazolone derivatives.
The band gap is computed by $E_{LUMO} - E_{HOMO}$

| Compounds | HOMO (eV) | LUMO (eV) | Band gap (eV) |
|---|---|---|---|
| P1 | -4.028 | -2.852 | 1.178 |
| P2 | -5.358 | -3.011 | 2.347 |
| P3 | -5.082 | -3.074 | 2.008 |
| P4 | -4.009 | -2.815 | 1.194 |
| P5 | -4.291 | -3.059 | 1.232 |
| P6 | -4.328 | -3.243 | 1.085 |
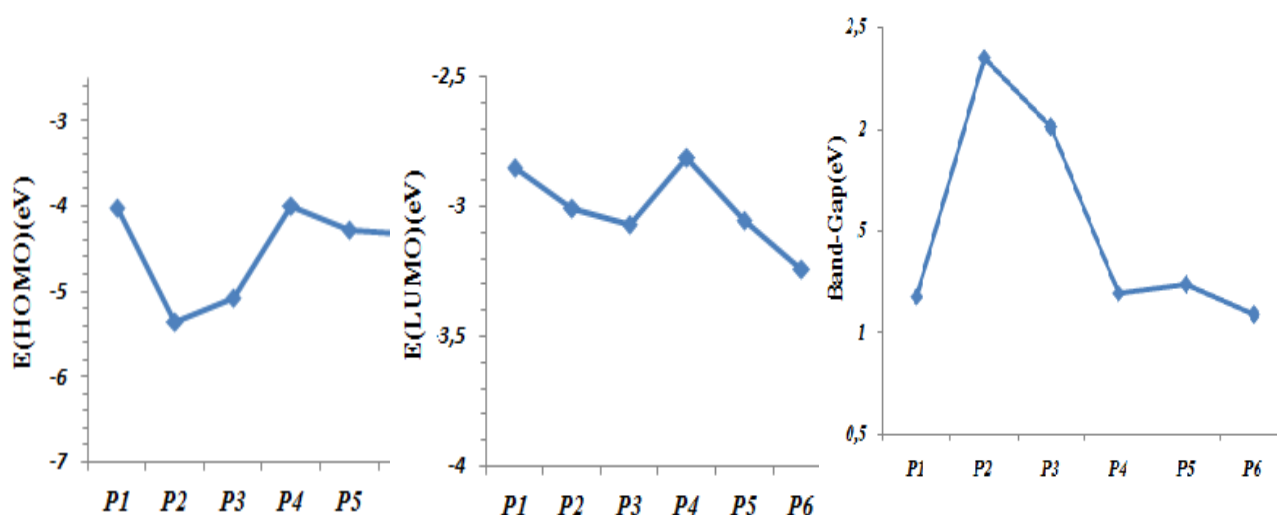
Fig. 2a            Fig. 2b            Fig. 2c

**Fig. 2.** Plot of highest occupied molecular orbitals, lowest unoccupied molecular orbitals, and band gap energies for P1 to P6

According to the Table 1, the gap energies increase from P6 to P2. This is due to the force of various acceptor groups given to the acceptor electron. Also, the HOMO/LUMO energies levels in consonance with the donor/acceptor of their electron are affected by the structure modification.

As mentioned previously, the HOMO and LUMO energies levels and band gap energies affect the photovoltaic performance of organic solar cells. The values of these energies levels are summarized in Table 1. The computational values of gap energies range from 1.085 to 2.347 eV.

It is clear from the Table 1 and Figure 2 that electron donating ability ($E_{HOMO}$) follows the order as P2 < P3 < P6 < P5 < P1 < P4 (Figure 2a).

Electron-accepting ability ($E_{LUMO}$) is seen to follow the order as P6 < P3 < P5 < P2 < P4 < P1 (Figure 2b).

What about the band gap from product P1to P6?

The chemical reactivity is highest and the kinetic stability is lowest for P6, P1 which is followed by P4, P5, P3 and P2 (Figure 2c). These proprieties are interesting to realize organic solar cells Hetero Junction.

Nonlinear optical (NLO) of P1 to P6

Intermolecular interactions the P1 to P6 are largely understood by DM, α, and first-order and second-order hyperpolarizability energy terms (Zhang et al., 2007), which are reliably computed by B3LYP/6-311G (d,p) level of the theory (Hurst et al., 2000; Gupta et al., 2017; El idrissi et al., 2019; Zeroual et al., 2017). How are these parameters affected for this compounds. To check this above basis set is used and dipole moments (DM), α, and first- and second-rank hyperpolarizability are determined (u.a). Isotropic DM ispresented in (Table 3).

**Table 3.** Cartesian components and net electric dipole moments (DM in Debye) for products P1 to P6

| Names | DMx | DMy | DMz | DM$_{Total}$ |
|---|---|---|---|---|
| P1 | 0.00 | 0.00 | 8.46 | 8.50 |
| P2 | 0.00 | 0.00 | 6.38 | 6.40 |
| P3 | 7.65 | 0.00 | 0.00 | 7.70 |
| P4 | 8.68 | 0.00 | 0.00 | 8.70 |
| P5 | 0.00 | 0.00 | 7.85 | 7.90 |
| P6 | 0.00 | 7.16 | 0.00 | 7.20 |

It is seen that the X and Y components are zero in all the cases with the Z component constituting the total $DM$. Higher and lower $DM_{TOTAL}$ than the reported mean value are highlighted in Table 3. Here, (P4, P1, P5) and (P3, P6, P2) show higher and lower $DM_{TOTAL}$, respectively.

The Polarizability (α), anisotropic (Δα), polarizability (β), hyperpolarizability <β> and isotropic β// values of P1 to P6products are given in Table 4. Few of these properties are also plotted in (Figure 3) (Figure 3a for α and Δα; Figure 3b for <β> and β//).

**Table 4.** Polarizability (α), anisotropic (Δα), polarizability (β), hyperpolarizability <β> and isotropic β// values of compounds P1 to P6 ( in $10^{-30}$ esu Unit).

| | Parameter | P1 | P2 | P3 | P4 | P5 | P6 |
|---|---|---|---|---|---|---|---|
| **\*Polarizability α \*anisotropic Δα** | $\alpha_{xx}$ | 31.25 | 35.91 | 30.25 | 34.88 | 32.35 | 29.56 |
| | $\alpha_{yx}$ | 9.65 | 10.25 | 7.65 | 8.65 | 7.16 | 8.97 |
| | $\alpha_{yy}$ | 29.87 | 33.21 | 30.26 | 31.54 | 30.83 | 32.01 |
| | $\alpha_{zx}$ | 10.31 | 11.23 | 12.81 | 10.22 | 11.2 | 9.56 |
| | $\alpha_{zy}$ | 9.36 | 10.25 | 12.74 | 9.87 | 10.55 | 8.59 |
| | $\alpha_{zz}$ | 58.26 | 64.78 | 43.44 | 50.22 | 51.36 | 51.63 |
| | $\alpha \times 10^{-24}$ **(esu)** | 39.79 | 44.63 | 34.65 | 38.88 | 38.18 | 37.73 |
| | **Δα** | 80.74 | 87.8 | 72.89 | 67.16 | 70.89 | 68.58 |
| **\*Hyperpolarizability <β> \* isotropic β//** | **βxxx** | 3.08 | 5.22 | 4.82 | -3.87 | 4.23 | -3.66 |
| | **βxxy** | 3.56 | -4.41 | 3.22 | 5.32 | 5.22 | 2.88 |
| | **βyxy** | 2.87 | 4.77 | -3.65 | 3.43 | -4.02 | 5.23 |
| | **βyyy** | 4.89 | -3.47 | -5.23 | -4.68 | 3.26 | 3.62 |
| | **βxxz** | 3.44 | -4.41 | 6.03 | 5.28 | 4.92 | 4.61 |
| | **βyxz** | -2.36 | 5.06 | 5.22 | -4.69 | -3.22 | 3.66 |
| | **βyyz** | 3.29 | 4.19 | 4.81 | 3.65 | 3.51 | -5.22 |
| | **βzxz** | -3.24 | 2.74 | -2.68 | 3.02 | 2.86 | 4.87 |
| | **βzyz** | 4.54 | -4.14 | 4.12 | 4.11 | 4.23 | -3.02 |
| | **βzzz** | -5.89 | 6.89 | 5.83 | 4.69 | -3.68 | 3.82 |
| | **<β>** | 13.29 | 18.73 | 16.87 | 14.65 | 13.91 | 7.99 |
| | **β//** | 4.97 | 1.01 | 5.94 | 4.46 | 5.94 | 2.38 |
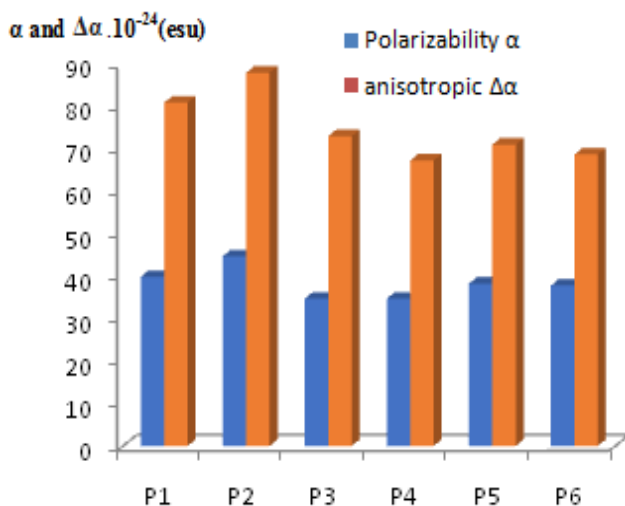
**Fig. 3a**
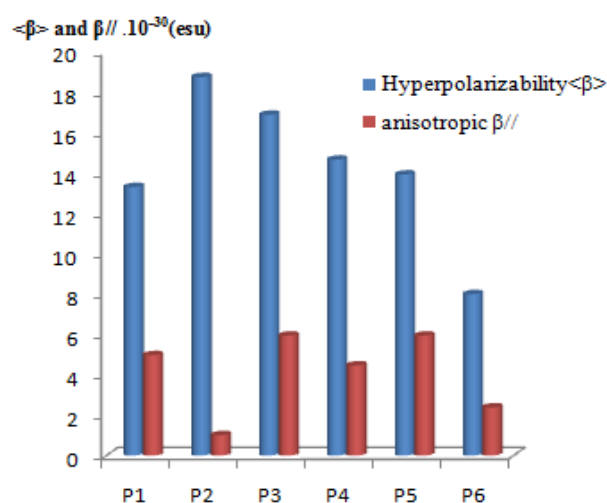
**Fig. 3b**

**Fig. 3.** Plot of polarizability (α), anisotropy of polarizability (Δα) (Figure 3a), hyperpolarizability <β> and isotropic β// (Figure 3b) for compounds P1 to P6

According to the data in (Table 1) the gap energies increase from $P_6$ to $P_2$ due to the force of various acceptor groups given to the acceptor electron. In addition, the HOMO/LUMO energy levels in agreement with the donor/acceptor of their electron are affected by the modification of the structure.

As mentioned previously, the HOMO and LUMO energies levels and band gap energies affect the photovoltaic performance of organic solar cells. The values of these energies levels are summarized in (Table 1). We can notice from these computational values of gap energies range from 1.085 to 2.347 eV.

The analysis of the results given in (Table 1) and (Figure 3) clearly shows in one hand that the electron donation capacity (EHOMO) follows the order as $P_2 < P_3 < P_6 < P_5 < P_1 < P_4$ (Figure 3a). On the other hand, the electron acceptance capacity (ELUMO) follows the order as $P_6 < P_3 < P_5 < P_2 < P_4 < P_1$ (Figure 3b).

### NBO analysis

The analysis of the results obtained in the study aimed at verifying that the DFT procedure was fulfilled. On doing it previously, several descriptors associated with the results that HOMO and LUMO calculations obtained are related with results obtained using the vertical I and A following the ΔSCF procedure. A link exists between the three main descriptors and the simplest conformity to the Koopmans' theorem by linking ϵH with -I, $\varepsilon_L$ with -A, and their behavior in describing the HOMO-LUMO gap as $JI = |\varepsilon_H + Egs(N-1) - Egs(N)|$, $JA = |\varepsilon_L + Egs(N) - Egs(N+1)|$ and $J_{HL} = \sqrt{J_I^2 + J_A^2}$. Notably, the JA descriptor consists of an approximation that remains valid only when the HOMO that a radical anion has (the SOMO) shares similarity with the LUMO that the neutral system has. Consequently, we decided to design an other descriptor ΔSL (the difference between the SOMO and LUMO energies), to guide in verifying how the approximation is accurate (Weigend et al., 2005; Pereira et al., 2017). The results of this analysis are presented in (Tables 5 to 10).

**Table 5.** Electronic energies of the neutral, positive and negative molecular systems (in au), the HOMO, LUMO, and SOMO orbital energies (in eV), JI, JA, JHL, and ΔSL descriptors (also in eV) calculated with DFT/B3LYB, CAM-B3LYP, HSEH1PBE, HCTH407 and WB97XD for compound P1

| | $E_0$ | $E^+$ | $E^-$ | HOMO | LUMO | SOMO | $J_i$ | $J_A$ | $J_{HL}$ | $\Delta S_L$ |
|---|---|---|---|---|---|---|---|---|---|---|
| **B3LYP** | -1402.064 | -1401.654 | -1402.458 | -4.028 | -2.852 | -3.885 | 14.748 | 14.008 | 20.341 | 1.033 |
| **CAM-B3LYP** | -1401.987 | -1401.512 | -1402.265 | -5.523 | -1.265 | -4.256 | 13.087 | 14.189 | 19.303 | 2.991 |
| **HSEH1PBE** | -1401.656 | -1401.482 | -1401.845 | -4.254 | -2.453 | -3.002 | 9.396 | 7.187 | 11.829 | 0.549 |
| **HCTH407** | -1401.438 | -1401.236 | -1401.654 | -4.365 | -2.688 | -3.258 | 10.242 | 8.184 | 13.11 | 0.570 |
| **WB97XD** | -1401.068 | -1399.879 | -1399.954 | -4.675 | -2.741 | -3.784 | 25.645 | 35.093 | 43.465 | 1.043 |

**Table 6.** Electronic energies of the neutral, positive and negative molecular systems (in au), the HOMO, LUMO, and SOMO orbital energies (in eV), JI, JA, JHL, and ΔSL descriptors (also in eV) calculated with DFT/B3LYB, CAM-B3LYP, HSEH1PBE, HCTH407and WB97XD for compound P2

| | $E_0$ | $E^+$ | $E^-$ | HOMO | LUMO | SOMO | $J_i$ | $J_A$ | $J_{HL}$ | $\Delta S_L$ |
|---|---|---|---|---|---|---|---|---|---|---|
| **B3LYP** | -1561.379 | -1561.723 | -1561.587 | -5.358 | -3.011 | -4.022 | 11.017 | 6.349 | 12.715 | 0.991 |
| **CAM-B3LYP** | -1561.164 | -1561.023 | -1561.364 | -6.235 | -1.998 | -5.236 | 11.677 | 5.834 | 13.053 | 3.238 |
| **HSEH1PBE** | -1560.886 | -1560.736 | -1561.087 | -5.624 | -3.225 | -3.854 | 11.093 | 7.306 | 13.282 | 0.629 |
| **HCTH407** | -1560.652 | -1560.523 | -1560.756 | -5.864 | -3.741 | -4.056 | 8.693 | 7.251 | 11.32 | 0.315 |
| **WB97XD** | -1560.365 | -1560.254 | -1560.546 | -5.744 | -3.994 | -4.158 | 10.669 | 7.014 | 12.768 | 0.464 |

**Table 7.** Electronic energies of the neutral, positive and negative molecular systems (in au), the HOMO, LUMO, and SOMO orbital energies (in eV), JI, JA, JHL, and ΔSL descriptors (also in eV) calculated with DFT/B3LYB, CAM-B3LYP, HSEH1PBE, HCTH407 and WB97XD for compound P3

| | $E_0$ | $E^+$ | $E^-$ | HOMO | LUMO | SOMO | $J_i$ | $J_A$ | $J_{HL}$ | $\Delta S_L$ |
|---|---|---|---|---|---|---|---|---|---|---|
| **B3LYP** | -1723.247 | -1723.621 | -1723.487 | -5.082 | -3.074 | -4.179 | 11.612 | 7.102 | 13.612 | 1.105 |
| **CAM-B3LYP** | -1723.087 | -1723.456 | -1723.254 | -6.357 | -1.023 | -5.214 | 10.901 | 9.017 | 14.147 | 4.191 |
| **HSEH1PBE** | -1722.874 | -1723.145 | -1723.183 | -5.231 | -2.987 | -3.587 | 13.638 | 4.386 | 14.327 | 0.601 |
| **HCTH407** | -1722.587 | -1722.883 | -1722.897 | -5.876 | -3.245 | -4.011 | 14.311 | 4.809 | 15.097 | 0.766 |
| **WB97XD** | -1722.752 | -1722.741 | -1722.756 | -5.001 | -3.667 | -4.572 | 5.109 | 3.966 | 6.468 | 0.905 |

**Table 8.** Electronic energies of the neutral, positive and negative molecular systems (in au), the HOMO, LUMO, and SOMO orbital energies (in eV), JI, JA, JHL, and ΔSL descriptors (also in eV) calculated with DFT/B3LYB, CAM-B3LYP, HSEH1PBE, HCTH407 and WB97XD for compound P4

| | $E_0$ | $E^+$ | $E^-$ | HOMO | LUMO | SOMO | $J_i$ | $J_A$ | $J_{HL}$ | $\Delta S_L$ |
|---|---|---|---|---|---|---|---|---|---|---|
| **B3LYP** | -1568.746 | -1568.969 | -1568.762 | -4.009 | -2.815 | -3.219 | 4.444 | 3.252 | 5.507 | 0.404 |
| **CAM-B3LYP** | -1568.523 | -1568.621 | -1568.587 | -5.674 | 1.775 | -4.236 | 7.415 | 4.441 | 8.643 | 2.461 |
| **HSEH1PBE** | -1568.311 | - | - | -4.236 | -2.546 | -3.578 | 6.303 | 0.474 | 6.321 | 1.032 |

| | | 1568.422 | 1568.387 | | | | | | | |
|---|---|---|---|---|---|---|---|---|---|---|
| **HCTH407** | -1568.186 | -1568.321 | -1567.265 | -4.701 | -2.312 | -3.256 | 20.359 | 1.361 | 20.404 | 0.056 |
| **WB97XD** | -1567.887 | -1568.077 | -1566.756 | -4.887 | -2.905 | -3.876 | 25.887 | 2.264 | 25.986 | 0.971 |

**Table 9.** Electronic energies of the neutral, positive and negative molecular systems (in au), the HOMO, LUMO, and SOMO orbital energies (in eV), JI, JA, JHL, and ΔSL descriptors (also in eV) calculated with DFT/B3LYB, CAM-B3LYP, HSEH1PBE, HCTH407 and WB97XD for compound P5

| | $E_0$ | $E^+$ | $E^-$ | HOMO | LUMO | SOMO | $J_i$ | $J_A$ | $J_{HL}$ | $\Delta S_L$ |
|---|---|---|---|---|---|---|---|---|---|---|
| **B3LYP** | -1528.419 | -1528.845 | -1528.689 | -4.291 | -3.059 | -3.547 | 11.637 | 8.532 | 14.43 | 0.488 |
| **CAM-B3LYP** | -1528.209 | -1528.546 | -1528.458 | -3.256 | -2.009 | -2.658 | 10.031 | 7.16 | 12.324 | 0.649 |
| **HSEH1PBE** | -1528.025 | -1528.126 | -1528.087 | -4.215 | -3.546 | -3.951 | 5.902 | 0.797 | 5.955 | 0.405 |
| **HCTH407** | -1527.886 | -1528.056 | -1527.911 | -4.985 | -3.987 | -4.031 | 5.665 | 0.638 | 5.701 | 0.044 |
| **WB97XD** | -1527.621 | -1527.833 | -1527.725 | -5.023 | -4.002 | -4.552 | 7.852 | 1.766 | 8.049 | 0.550 |

**Table 10.** Electronic energies of the neutral, positive and negative molecular systems (in au), the HOMO, LUMO, and SOMO orbital energies (in eV), JI, JA, JHL, and ΔSL descriptors (also in eV) calculated with DFT/B3LYB, CAM-B3LYP, HSEH1PBE, HCTH407 and WB97XD for compound P6

| | $E_0$ | $E^+$ | $E^-$ | HOMO | LUMO | SOMO | $J_i$ | $J_A$ | $J_{HL}$ | $\Delta S_L$ |
|---|---|---|---|---|---|---|---|---|---|---|
| **B3LYP** | -1515.384 | -1515.786 | -1515.548 | -4.328 | -3.243 | -3.985 | 8.79 | 7.695 | 11.682 | 0.742 |
| **CAM-B3LYP** | -1515.214 | -1515.544 | -1515.355 | -4.008 | -2.008 | -3.879 | 7.844 | 6.971 | 10.494 | 1.871 |
| **HSEH1PBE** | -1515.018 | -1515.315 | -1515.245 | -3.987 | -3.654 | -3.801 | 10.163 | 4.427 | 11.086 | 0.147 |
| **HCTH407** | -1514.857 | -1515.095 | -1514.953 | -3.564 | -3.874 | -3.652 | 6.176 | 2.601 | 6.701 | 0.222 |
| **WB97XD** | -1514.687 | -1514.901 | -1514.766 | -3.148 | -3.212 | -3.012 | 5.297 | 2.61 | 5.906 | 0.201 |

The overall conclusion that can be extracted from the inspection of the results presented in Tables 5 to 10 is that in agreement with our previous studies on P1 to P6, the values of JI, JA, and JHL are actually not zero. Nevertheless, the results tend to be impressive especially for the CAM-B3LYB density functional. As well, the ΔSL descriptor reaches the minimum values when HSEH1PBE and HCTH107 density functional are used in the calculations. This implies that there are sufficient justifications to assume that the LUMO of the all products.
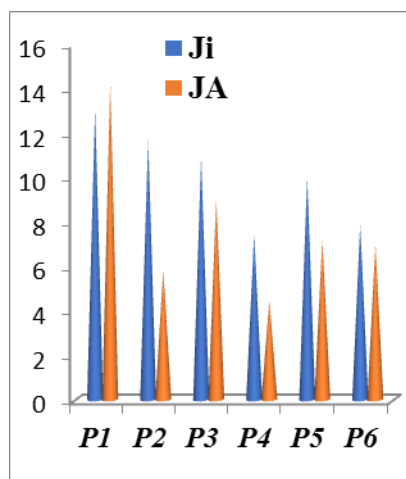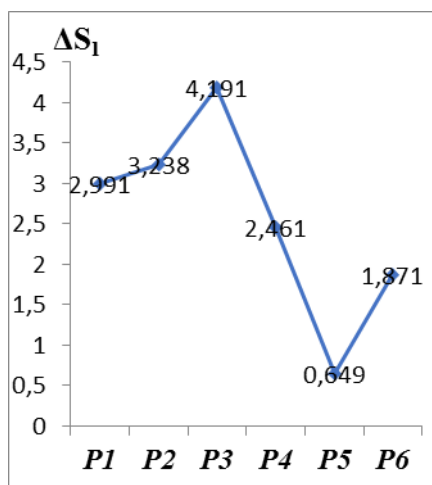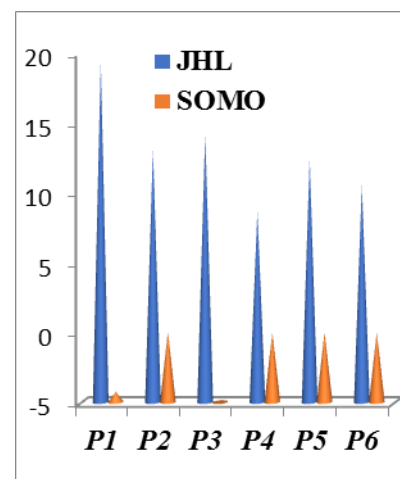
Fig. (4a)    Fig. (4b)    Fig. (4c)

**Fig. 4.** Plot of JA and JA descriptor (Figure 4a), ΔSL (Figure 4b), JHL and SOMO (Figure 4c) for compounds P1 to P6 by CAM-B3LYB

The values of *JI, JA,* and *JHL* are actually not zero. Nevertheless, the results tend to be impressive especially for the CAM-B3LYB density functional. As well, the ΔSL descriptor reaches the minimum values when HSEH1PBE and HCTH407 density functionals are used in the calculations. This implies that there are sufficient justifications to assume that the SOMO of the neutral approximates the electron affinity.

The analysis of the results given in (Tables 5 to 10) and (Figure 4) clearly shows in one hand that the JA and JA descriptor follows the order as $P_1 < P_3 < P_2 < P_5 < P_4 < P_6$ (Figure 4a). On the other hand, the ΔSL follows the stability is lowest for P3 and P2 products (Figure 4b).

## 4. Conclusion

In this paper, we have presented a new study performed on the chemical reactivity of P1 to P6 compounds on conceptual DFT as a tool to explain molecular interactions. The obtained results show that:

- The electron-accepting ability (ELUMO) is seen to follow the order as P6 < P3 < P5 < P2 < P4 < P1;

- (P4, P1, P5) and (P3, P6, P2) proudcuts show higher and lower DMTOTAL, respectively;

- The JA and JA descriptor follows the order as P1 < P3 < P2 < P5 < P4 < P6. On the other hand, the ΔSL follows the stability is lowest for P3 and P2 products.

## 5. Funding statement

## 6. Conflict of interest

The authors declare no conflict of interest.

## References

Aihara et al., 1999 - Aiharaб Jюl. (1999). Reduced HOMO-LUMO gap as an index of kinetic stability for polycyclic aromatic hydrocarbons. *J Phys Chem A.* 103: 7487-95.

Ameri, 2009 – Ameri, T., Dennler, G., Lungen schmied, C., Brabec, C. (2009). Organic solar cell design as a function of radiative quantum efficiency. *Energy Environ Sci.* 2: 347-363.

Bahadur, Srivastava, 2004 – Bahadur, L., Srivastava, P. (2004). Small molecular white organic light emitting devices with a single emission layer. *Semicond. Sci. Technol.* 19: 531.

Bahçeli et al., 2015 – Avcı, D., Bahçeli, S., Tamer, Ö., Atalay, Y. (2015). Comparative study of DFT/B3LYP, B3PW91, and HSEH1PBE methods applied to molecular structures and spectroscopic and electronic properties of flufenpyr and amipizone. *Can. J. Chem.* 93: 1147.

Becke, 1993 – *Becke, A.D.* (1993). A new mixing of Hartree-Fock and local density functional theories. *J. Chem. Phys.* 98: 1372.

Bhattacharjya et al., 2008 – *Jain, V., Rajbongshi, B.K., Tej Mallajosyula, A., Bhattacharjya, G., Iyer, S.S.K., Ramanathan, G.* (2008). Segregation into Chiral Enantiomeric Conformations of an Achiral Molecule by Concomitant Polymorphism. *Sol. Energy Mater. Sol. Cells.* 92 : 1043.

Boreland, 2008 – *Bagnall, D.M., Boreland, M.* (2008). Photovoltaic technologies. *Energy policy.* 36: 4390-4396.

Chen et al., 2017 – *Chen, L., Lu, J., Huang, T., Cai, Y.D.* (2017). A computational method for the identification of candidate drugs for non-small cell lung cancer. *PLoS One.* 12: e0183411.

Chuang et al., 2009 – *Chuang, W.T., Chen, B.S., Chen, K.Y., Hsieh, C.C., Chou, P.T.* (2009). Fluorescent protein red Kaede chromophore; one-step, high-yield synthesis and potential application for solar cells. *Chem. Commun.* 6982.

Desharnais et al., 2003 – *Boger, D.L., Desharnais, J., Capps, K.* (2003). Solution-phase combinatorial libraries: Modulating cellular signaling by targeting protein-protein or protein-DNA interactions. *Angew Chem Int Ed Engl.* 42: 4138-76.

El idrissi et al., 2019 – *Zeroual, A., Ríos-Gutiérrez, M., El Alaoui El Abdallaoui, H., Domingo L.R.* (2019). An MEDT study of the mechanism and selectivities of the [3 + 2] cycloaddition reaction of tomentosin with benzonitrile oxide. *Int J Quantum Chem.* 1(1): 1-9.

Francl, 1982 – *Francl, M.M., Pietro, W.J., Hehre, W.J.J.* (1982). Self-Consistent Molecular Orbital Methods. XXIII. A Polarization-Type Basis Set for Second-Row Elements. *Chem. Phys* .77: 3654-3665.

Frisch et al., 2009 – *Frisch, J., Trucks, G.W., Schlegel, H.B. et al.* (2009). Gaussian 09, Revision a.1, Gaussian, Inc., Wallingford, CT.

Ghanadzadeh et al., 2000 – *Ghanadzadeh, A., Ghanadzadeh, H., Ghasmi G.* (2000). On the molecular structure and aggregative properties of Sudan dyes in the anisotropic host. *J. Mol. Liq.* 88: 299-308.

Green et al., 2009 – *Green, M., Emery, K., Hishikawa, Y., Warta, W.* (2009). Solar Power Generation: Technology, New Concepts & Policy. *Prog Photovol Res Appl.* 17: 320-326.

Gupta et al., 2017 – *Ansary, I., Das, A., Gupta, P.S., Bandyopadhyay, A.K.* (2017). Synthesis, molecular modeling of N-acyl benzoazetinones and their docking simulation on fungal modeled target. *Synth Commun.* 47: 1375-1386.

Hadipour, 2008 – *Hadipour, A., de Boer, B., Blom, P.* (2008). Organic tandem and multi-junction solar cells. *Adv Funct Mater.* 18: 169-181.

Hansch et al., 2003 – *Hansch, C., Steinmetz, W.E., Leo, A.J., Mekapati, S.B., Kurup, A., Hoekman D.* (2003). On the role of polarizability in chemical-biological interactions. *J. Chem Inf Comput Sci.* 43: 120-5.

Harris et al., 1999 – *Harris, P.G., Baker, C.A., Green, K., Iaydjiev, P., Ivanov, S., May, D.J.* (1999). New experimental limit on the electric dipole moment of the neutron. *Phys Rev Lett.* 82: 904.

Hurst et al., 2000 – *Hurst, G.J., Dupuis, M., Clementi, E.* (2000). A binitio analytic polarizability, first and second hyperpolarizabilities of large conjugated organic molecules: Applications to polyenes $C_4H_6$ to $C_{22}H_{24}$. *J. Chem Phys.* 89: 385-95.

Kim et al., 2005 – *Reyes-Reyes, M., Kim, K., Carroll, D.* (2005). Origins of performance in fiber-based organic photovoltaics. *Appl Phys Lett.* 87: 083506.

Lee, 2007 – *Kim, J., Lee, K., Coates, N., Moses, D., Nguyen, T., Dante, M., Heeger, A.* (2007). Organic, Inorganic and Hybrid Solar Cells: Principles and hybrid Solar Cells. *Science.* 317: 222-225.

Lim et al., 1999 – *Lim, I.S., Pernpointner, M., Seth, M., Laerdahl, J.K., Schwerdtfeger, P., Neogrady, P.* (1999). Relativistic coupled-cluster static dipole polarizabilities of the alkali metals from Li to element 119. *Phys Rev A.* 60: 2822.

Lu et al., 2015 – *Lu, L., Kelly, M.A., You, W., Yu, L.* (2015). Status and prospects for ternary organic photovoltaics. *Nat. Phot.* 9: 491e500.

Obot et al., 2009 – *Obot, I.B., Obi-Egbedi, N.O., Umoren, S.A.* (2009). Antifungal drugs as corrosion inhibitors for aluminium in 0.1 M HCl. *Corrosion Science.* 51(8): 1868-75.

Park et al., 2009 – *Park, S., Roy, A., Beaupré, S., Cho, S., Coates, N.E., Moon, J., Moses, D., Leclerc, M., Lee, K., Heeger,* A. (2009). Polymer Photovoltaics: Materials, Physics and Device Enginee. *Nat. Photon.* 3: 297-302.

Pereira et al., 2017 – *Pereira, T.L., Leal, L.A., da Cunha, W.F., Timóteo de Sousa, R., Ribeiro Junior, L.A. et al.* (2017). Optimally tuned functionals improving the description of optical and electronic properties of the phthalocyanine molecule. *J. Mol. Model.* 23: 71.

Weigend et al., 2005 – *Weigend, F., Ahlrichs, R.* (2005). Balanced basis sets of split valence, triple zeta valence and quadruple zeta valence quality for H to Rn: design and assessment of accuracy. *Phys. Chem. Chem. Phys.* 7: 3297-3305.

Xue et al., 2004 – *Xue, Y., Li, Z.R., Yap, C.W., Sun, L.Z., Chen, X., Chen, Y.Z.* (2004). Effect of molecular descriptor feature selection in support vector machine classification of pharmacokinetic and toxicological properties of chemical agents. *J Chem Inf Comput Sci.* 44: 1630-8.

Yang et al., 2005 – *Ma, W., Yang, C., Gong, X., Lee, K., Heeger, A.* (2005). Thermally Stable, Efficient Polymer Solar Cells with Nanoscale Control of the Interpenetrating Network Morphology. *Adv Funct Mater.* 15: 1617-1622.

Yang, 1988 – *Lee, C.T., Yang, W.T, Parr, R.G.* (1988). Density-functional exchange energy approximation with correct asymptotic behavior. *Physical Review B.* (37): 785-89.

You et al., 2000 – *You, Y., He, Y., Burrows, P.E., Forrest, S.R., Petasis, N.A., Thompson, M.E.* (2000). Tuning the solid-state emission of the analogous GFP chromophore by varying alkyl chains in the imidazolinone ring. *Adv. Mater.* 12: 1678.

Zeroual et al., 2017 – *Zoubir, M., Zeroual, A., El Idrissi, M., Bkiri, F., Benharref, A., Mazoir, N., El Hajbi, A.* (2017). Experimental and theoretical analysis of the reactivity and regioselectivity in esterification reactions of diterpenes (totaradiol, totaratriol, hinikione and totarolone). *Mediterranean Journal of Chemistry.* 6(4): 98-107.

Zhan et al., 2003 – *Zhan, C.G., Nichols, J.A., Dixon, D.A.* (2003). Ionization potential, electron affinity, electronegativity, hardness, and electron excitation energy: Molecular properties from density functional theory orbital energies. *J. Phys Chem A.* 107: 4184-4195.

Zhang et al., 2007 – *Zhang, C., Song Y.L., Wang. X.* (2007). Correlations between molecular structures and third-order non-linear optical functions of heterothmetallic clusters: a comparative study. *Chem. Reviews.* 251: 1-2.

# Applications of EVODROP Water as Drinking Water of Highest Quality. Antibacterial and Antiviral Effects of EVOhygiene Colloidal Silver and Cooper Nano Water

Fabio Huether [a], Ignat Ignatov [b, *], Nedyalka Valcheva [c], Georgi Gluhchev [d]

[a] EVODROP AG, Zürich, Switzerland
[b] Scientific Research Center of Medical Biophysics (SRCMB), Sofia, Bulgaria
[c] Trakia University, Stara Zagora, Bulgaria
[d] Bulgarian Academy of Sciences (BAS), Sofia, Bulgaria

## Abstract

Scientific evidence of Ignat Ignatov and Oleg Mosin show that in the mountain areas in Bulgaria, where the scientific and practical project "Nature, Ecology, Longevity" is held, one can meet 104 years old centenarians. In the field areas at a distance of only about 50-70 km, the oldest person is 97 years old. We have reasons to give these facts some thought. The difference is in the water, the air and the physical activity. In the mountains people drink water from springs. This water is "active". When you drink water from the source itself, the water molecules are more dynamic and it is "tastier, more energy-filled and more alive". In biophysics it is known that movement is life. Therefore, people who are active, live longer. They also feel the water more strongly, a water that is like an elixir even after the first sips from the spring. Everyone should ask themselves: "How can we have such water in our homes?" The research shows that tap water has low level of energy of hydrogen bonds among water molecules.

**Keywords:** EVOhygiene Colloidal Silver and Cooper, microbiological parameters, spectral analyses NES and DNES.

## 1. Introduction

Studies reveal that in cases of longevity, the water consumed by long-living people is with high energies of hydrogen bonds from one water molecule and oxygen from another one. Mountain and glacier waters are of high quality. With the highest possible quality is EVODROP Water gained from a device with author Fabio Huether, which can easily be acquired in everybody's home. EVODROP Water is water of highest quality that provides in your home the energy and freshness of the mountain and glacier waters.

The research of water clusters $(H_2O)_n$ are with the following methods ^{1}H-NMR, neurons diffraction, X-Ray, EXAFS-spectroscopy, IR spectroscopy, NES and DNES spectral methods. There ionic clusters $[(H_2O)_n]^+$ and $[(H_2O)_n]^-$.

In this research two of the authors Ignatov and Gluhchev have performed mathematical models of water molecules of EVODROP water and tap water.

The following parameters of EVODROP water – spectral parameters, hardness, oxidation reduction potential (ORP) and pH are studied.

---

* Corresponding author
E-mail addresses: mbioph@abv.bg (I. Ignatov)

There are proofs for the effects of different types of drinking wates on human longevity (Ignatov et al., 2014–2018), antitumor effects (Toshkova et al., 2019), anti-bacterial and anti-viral effects (Valcheva et al., 2014–2020; Karadzhov et al., 2014–2015).

The aim of research is to show the Applications of EVODROP Water as Drinking Water of Highest Quality. The Antibacterial and Antiviral Effects of EVOhygiene Colloidal Silver and Cooper Nano Water were studied.

## 2. Methods

### 2.1. NES and DNES Spectral Analyses

The device invented by A. Antonov, based on an optical principle and methods NES and DNES for spectral analysis are used. The evaporation of water drops is in hermetic camera with a glass plate and water-proof transparent pad which consists of thin maylar folio.

The parameters are:

- monochromatic filter with wavelength $\lambda$ = 580±7 nm (yellow color in visible spectrum);
- angle of evaporation of water drops from 72.3° to 0°;
- temperature (+22–24 °C);
- range of energy of hydrogen bonds among water molecules is $\lambda$ = 8.9–13.8 μm or
- E=-0.08– -0.1387 eV.;

The energy ($E_{H...O}$) of hydrogen O...H-bonds among $H_2O$ molecules in water sample is measured in eV. The function f(E) is called a spectrum of energues distribution. The energy spectrum of water is characterized by a non-equilibrium process of water droplets evaporation and this is a non-equilibrium energy spectrum (NES), measured in $eV^{-1}$. DNES is defined as the difference

$\Delta f(E) = f$ (samples of water) – $f$ (control sample of water),

where $f(*)$ denotes the evaluated energy.

DNES is measured in $eV^{-1}$ as well.

### 2.2. Electrical measurements

The device – HANNA Instruments HI221 meter equipped with Sensorex sensors was used for the measurement of Oxidation Reductin Potental (ORP) in mV, and pH.

The Range of HANNA Instruments HI221 meter is:

pH - (2.00-16.00 ±0.01)

ORP (±699.9±0.01 − ±2000±0.1) mV

### 2.3. Concentration of EVODROP Silver Nanoparticle in sample with bacteria

The concentration is 500 mL EVODROP Silver Nanoparticle with 30 ppm and 500 mL control sample with bacteria.

In the materials and methods are including nutrient media and methods for determination of microbiological indicators.

### 2.4. Nutrient media

1. Nutrient agar (MPA) with contents (in %) – meat water, peptone – 1%, agar –agar – 2 % . Endo's Medium (for defining of *Escherichia coli* and *coliform* bacteria) with contents (g/dm³) – peptone– 5,0 ;triptone– 5,0; lactose – 10,0; $Na_2SO_3$ – 1,4; $K_2HPO_4$– 3,0; fuchsine– 0,14; agar – agar– 12,0 pH 7,5 – 7,7 .

2. Nutrient gelatine (MPD) (for defining of *Pseudomonas aeruginosa*) with contents (in %) – Peptic digest of animal tissue; 25 % gelatin ;pH = 7, 0 – 7, 2.

3. Medium for defining of enterococci (esculin – bile agar).

4. Medium for defining of sulphite reducing bacteria (Iron Sulfite Modified Agar).

5. Wilson-Bleer medium (for defining of sulphite reducing spore anaerobes (*Clostridium perfringens*) with contents(g/dm³) – 3 % Nutrient agar; 100 cm³20% solution $Na_2SO_3$; 50 cm³ 20 % glucose solution; 10 cm³ 8 % solution of$Fe_2SO_4$.

### 2.5. Methods for determination of microbiological indicators

1. Methods for evaluation of microbiological indicators according to Ordinance № 9/2001, Official State Gazette, issue 30, and decree № 178 / 23.07.2004 about the quality of water, intended for drinking purposes.

2. Method for determination of *Escherichia coli* and coliform bacteria –BDSEN ISO 9308 – 1: 2004;

3. Method for determination of enterococci – BDS EN ISO 7899 – 2;

4. Method for determination of sulphite reducing spore anaerobes – BDS EN 26461 – 2: 2004;

5. Method for determination of total number of aerobic and facultative anaerobic bacteria – BDS EN ISO 6222: 2002;

6. Method for determination of *Pseudomonas aeruginosa* – BDS EN ISO 16266: 2008.

7. Determination of coli – titre by fermentation method – Ginchev's method

Determination of coli – bacteria over Endo's medium – membrane method.

8. Determination of sulphite reducing anaerobic bacteria (*Clostridium perfringens*) – membrane method.

### 3. Results
### 3.1. Results with spectral methods NES and DNES

The Table 1 shows the local extremum at 8.95 μm. Such a local extremum is connected to the state of water molecules in longevity. It is decreasing in tumor diseases.

**Table 1.** Comparative analyses between EVODROP water and other waters

| Type of Water | Value eV $^{-1}$ of Local Extremum at (-0.1362– -0.1387) | (%((-Evalue) */ (-Etotal value)** |
|---|---|---|
| Deionized water | 18.2±1.2 | 4.5 |
| Mountain water from Vasiliovska mountain, Bulgaria | 44.9±2.2 | 11.2 |
| Northern Rhodope | 59.3±3.0 | 18.5 |
| Glasier Rosenlaui, Switzerland | 70.1±3.5 | 19.4 |
| Glasier Mappa, Chile | 81.3±4.1 | 20.1 |
| Tap water from Zurich before EVODROP device | 38.3±1.9 | 16.0 |
| EVODROP drinking water | 89.9±4.5 | 25.5 |

* The result (-$E_{value}$) is the result of hydrogen bonds energy for one parameter of (-E)
** The result (-$E_{total\ value}$) is the total result of hydrogen bonds energy

The mathematical model of the EVODROP water gives us information about the structuring of water clusters with sizes of up to 3 nanometers. Those clusters are with larger and with higher energies than the clusters of tap water. The analysis is based on a mathematical model established in 2013 by Ignatov and Mosin. The model was adopted in modern science, together with the evidence of Richard Saykally of Berkeley College of Chemistry.

A mathematical model of the number of water molecules according to the energy of hydrogen bonds in EVODROP water has been developed (Ignatov, Gluhchev, 2020) (Table 2; Figure 1).

The definition of the author of Nano clusters of EVODROP Fabio Huether is EVODROP® Water.

The mathematical model of EVODROP water show stable clusters between 3 and 25 water molecules.

**Table 2.** Distribution of the number of water (H₂O) molecules in EVODROP water according to the energy of hydrogen bonds

| -E(eV)x-axis | EVODROP® Water Number of water molecules | Tap water (Control Sample) Number of water molecules | -E(eV)x-axis | EVODROP® Water Number of water molecules | Tap water (Control Sample) Number of water molecules |
|---|---|---|---|---|---|
| 0.0912 | 0 | 7 | 0.1162 | 0 | 0 |
| 0.0937 | 0 | 0 | 0.1187 | 3 | 8 |
| 0.0962 | 5 | 8 | 0.1212 | 15 | 0 |
| 0.0987 | 3 | 0 | 0.1237 | 0 | 5 |

| 0.1012 | 0 | 8 | 0.1262 | 0 | 5 |
|--------|---|---|--------|----|----|
| 0.1037 | 0 | 6 | 0.1287 | 9 | 7 |
| 0.1062 | 9 | 8 | 0.1312 | 2 | 4 |
| 0.1087 | 0 | 7 | 0.1337 | 0 | 5 |
| 0.1112 | 12 | 0 | 0.1362 | 17 | 8 |
| 0.1137 | 0 | 5 | 0.1387 | 25 | 14 |
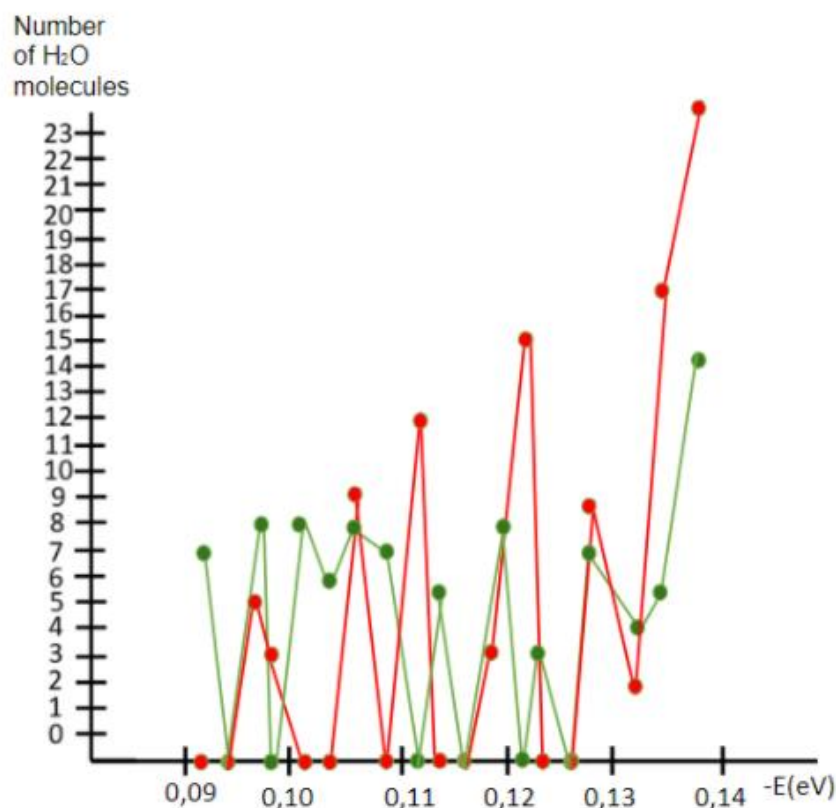


**Fig. 1.** Distribution of the number of water ($H_2O$) molecules in EVODROP water (red color) and tap water as control sample (green color) according to the energy of hydrogen bonds

### 3.2. Properties of EVODROP water

The water created by EVODROP water can be defined as nano-water or water of the future. It is has even better properties than mountain and glacier waters, and everyone can have it in their home. Tables 1 and 2 show that EVODROP water achieves by far the best values. EVODROP water even beats renowned glacier water, which we know to be of the best quality, as confirmed by numerous scientists such as Gerald Pollack, Mu Shik Jhon, Emilio Del Giudice and many others. The evidence-based and scientific proof is that EVODROP water is much better than natural glacier or spring water. It is the best water we have ever tested worldwide!

Ignatov proves that mountain water is unique to longevity, but can we always have this water in our homes?

The new chance in today's world is EVODROP water.

It is important that the EVODROP water is alkaline, and the alkalinity of the medium inhibits the development of tumor cells. EVODROP water activates free electrons with antioxidant activity. It is an elixir of youth as the antioxidant activity is one of the secrets for health and longevity, vitality, and energy. How can we describe longevity? In DNA replication we have doubling of the cells. This is obtained from one mother to two daughter cells. Errors are accumulated in the copy process. The fewer the mistakes, the longer the person lives. With the accumulation of a large number of errors, the number of tumor cells is activated. Essential is the impact on DNA replication on free radicals and the environment in which the replication is performed – water.

### 3.3. Study of pH and ORP of samples of EVODROP water

The research was performed from one of co-authors Georgi Gluhchev

The obtained results are shown in the following Table 3.

**Table 3.** Values of pH and ORP for EVODROP water

| EVODROP water values | ORP (mV) Sample EVODROP water | ORP (mV) Control Sample Tap water | ORP (mV) Sample minus Control Sample | pH Sample EVODROP water | pH Control Sample Tap water | pH Sample minus Control Sample |
|---|---|---|---|---|---|---|
| | +80 | +320 | -240 | 6.54 | 7.78 | -1.24 |

### 3.4. Research of hardness of EVODROP water

The parameter of hardness of tap water from Zurich is 7.82±0.39 mgeqv/l. The hardness of EVODROP water is 7.02±0.35 mgeqv/l. The difference 7.82-7.02=0.8±0.04 shows effect of decreasing of hardness of tap water from the device for EVODROP water.

This effect is ecential for human health for cardio vascular system.

### 3.5. Antibacterial properties of the EVOhygiene

Tests were performed of the antibacterial effects of the EVOhygiene by Nedyalka Valcheva, Trakia University, Stara Zagora, Bulgaria. The control sample water is in Table 4 (after 24 hours) and Table 5 (after 48 hours).

**Table 4.** Control sample of water with pathogens. Results after 24 hours

| Controlled parameter | Limit value, cfu/cm3 | Result, cfu/cm$^3$ |
|---|---|---|
| Coliforms | 0/100 | 7/100 |
| Escherichia coli | 0/100 | 7/100 |
| Enterococci | 0/100 | 4/100 |
| Sulphite reducing anaerobic bacteria (Clostridium perfringens) | 0/100 | 0/100 |
| Total number of microorganisms at 22 °C | 100 | 110 |
| Total number of microorganisms at 37 °C | 20 | 30 |
| Pseudomonas aeruginosa | 0/250 | 0/250 |

**Table 5.** Control sample of water with pathogens. Results after 48 hours

| Controlled parameter | Limit value, cfu/cm3 | Result, cfu/ cm$^3$ |
|---|---|---|
| Coliforms | 0/100 | 15/100 |
| Escherichia coli | 0/100 | 15/100 |
| Enterococci | 0/100 | 10/100 |
| Sulphite reducing anaerobic bacteria (Clostridium perfringens) | 0/100 | 0/100 |
| Total number of microorganisms at 22 °C | 100 | 120 |
| Total number of microorganisms at 37 °C | 20 | 50 |
| Pseudomonas aeruginosa | 0/250 | 0/250 |

The results with EVOhygiene are in Table 6 (after 24 hours) and Table 7 (after 48 hours).

**Table 6.** Results with EVOhygiene. Results after 24 hours

| Controlled parameter | Limit value, cfu/cm3 | Result, cfu/cm³ |
|---|---|---|
| Coliforms | 0/100 | 0/100 |
| Escherichia coli | 0/100 | 0/100 |
| Enterococci | 0/100 | 0/100 |
| Sulphite reducing anaerobic bacteria (Clostridium perfringens) | 0/100 | 0/100 |
| Total number of microorganisms at 22 °C | 100 | 0 |
| Total number of microorganisms at 37 °C | 20 | 0 |
| Pseudomonas aeruginosa | 0/250 | 0/250 |

**Table 7.** Results with EVOhygiene. Results after 24 hours

| Controlled parameter | Limit value, cfu/cm3 | Result, cfu/cm³ |
|---|---|---|
| Coliforms | 0/100 | 0/100 |
| Escherichia coli | 0/100 | 0/100 |
| Enterococci | 0/100 | 0/100 |
| Sulphite reducing anaerobic bacteria (Clostridium perfringens) | 0/100 | 0/100 |
| Total number of microorganisms at 22 °C | 100 | 3 |
| Total number of microorganisms at 37 °C | 20 | 3 |
| Pseudomonas aeruginosa | 0/250 | 0/250 |

The research shows anti-bacterial effects of EVOhygiene with Coliforms, Escherichia coli, Sulphite reducing anaerobic bacteria (*Clostridium perfringens*) and Pseudomonas aeruginosa.

**3.6. Antiviral effects of the EVOhygiene Nanoparticle Water.**

The nano colloidal silver with size of 5-20 nm of $Ag^+$ has got inhibiting effect over respiratory enzymes of the micro-organisms by building into the reaction center of the enzymes. Thus, it prevents the further alteration of the enzymes (Dondysh, 1964). Colloidal silver from the EVOhygiene makes physical changes in the bacterial membrane, like the membrane damage, which can lead to cellular contents leakage and bacterial death in interact with, and potentially disturb the functioning of bio molecules such as proteins and enzymes (Mosin, Ignatov, 2013). The coronavirus replicase was recently predicted to employ a variety of RNA processing enzymes. The colloidal silver $Ag^+$ inhibits such copying of the enzyme RNA-dependent RNA polymerase. In, and in this way are neutralized the effects of SARS-CoV-2, and thereby the effects of COVID-2019 are counteracted.

The colloidal silver of EVOhygiene is therefore absolutely safe for humans, animals and the environment. It does not harm, but supports humans, animals and even plants of all kinds in cell activation, immune system, stem cell formation, inflammation inhibition and much more. EVOhygiene colloidal silver is by far the safest, purest, and most effective for universal protection.

## 4. Conclusion

The basic conclusion from the research is that EVODROP water increases the average energy of hydrogen bonds among water molecules treatment compared to the average energy of hydrogen bonds among water molecules in control sample of tap water.

The mathematical models of EVODROP water give significant information about the possible number of hydrogen bonds as a percent of $H_2O$ molecules with different distribution of energy relative to the same number in control sample of tap water.

As a result of different energies of hydrogen bonds, the surface tension of EVODROP water is increased after the treatment relative to the control sample. This effect is connected with the preservation and increase in the energy of the biochemical processes between water molecules and biomolecules.

The following effects from the analysis of the local extremums in spectrum are valid:

1. Stimulating effect on nervous system and improvement of nervous conductivity.
2. Anti inflammatory effect.
3. Inhibition of development of tumor cells of molecular level.

The research was performed of EVOhygiene Colloidal Silver and Cooper ppm 30 with author Fabio Huether of microbiological effects of the following bacteria – *Escherichia coli, Enterococci, Coliforms, Clostridium perfringens.*

## References

Aider et al., 2012 – *Aider, M., Kastyuchik, A., Gnatko, E., Benali, M., Plutakhin, G.* (2012) Electro-activated Aqueous Solutions: Theory and Application in the Foodindustry and Biotechnology. *Innovative Food Science and Emerging Technologies.* 15: 38-49

Bakhir et al., 2001 – *Bakhir, V.M., Zadorozhnii, Y.G., Leonov, V.I., Panicheva, S.A., Prilutsky, V.I.* (2001). Electrochemical Activation; Water Purification and Production of Useful Solutions. *Moscow:VNIIIMT.* 1: 100-176.

Bachir, Pogorelov, 2018 – *Bachir, V.M., Pogorelov, A.G.* (2018). Universal Electrochemical Technology for Environmental Protection, *International Journal of Pharmaceutical Research & Allied Sciences.* 7(1): 41-57.

Cha, Chun-Nam et al., 2016 – *Cha, Chun-Nam et al.* (2016). Virucidal Efficacy of a Fumigant Containing Orth-phenylphenol Against Classical Swine Fever Virus and Porcine Reproductive and Respiratory Syndrome Virus. *Korean Journal of Veterinary Service.* 39(2): 117-124.

Fukuzaki, 2006 – *Fukuzaki, S.* (2006). Mechanisms of Actions of Sodium Hypochlorite in Cleaning and Disinfection Processes. *Biocontrol Sci.* 11(4): 147-57.

Gluhchev et al., 2015 – *Gluhchev, G., Ignatov, I., Karadzhov, S., Miloshev, G., Ivanov, N., Mosin, O.V.* (2015). Electrochemically Activited Water. Biophysical and Biological Effects of Anolyte and Catholyte as Types of Water. *Journal of Medicine, Physiology and Biophysics.* 10: 1-17.

Hoeijmakers, 2009 – *Hoeijmakers, J.H.* (2009). DNA Damage, Aging, and Cancer, 361(15): 1475-85.

Ignatov, Mosin, 2013 – *Ignatov, I., Mosin, O.V.* (2013). Structural Mathematical Models Describing Water Clusters. *Journal of Mathematical Theory and Modeling.* 3 (11): 72-87.

Ignatov et al., 2019 – *Ignatov, I., Toshkova, R., Gluhchev, G., Drossinakis, Ch.* (2019). Results of Blood Serum from Cancer Treated Hamsters with Infrared Thermal Field and Electromagnetic Fields. *Journal of Health, Medicine and Nursing.* 58: 101-112.

Antonov, 1995 – *Antonov, A.* (1995). Research of Nonequilibrium Processes in the Area of Allocated Systems. *Diss. Thesis Doctor of Physical Sciences*, 1-255.

Ignatov et al., 1998 – *Ignatov, I., Antonov, A., Galabova, T.* (1998). Medical Biophysics – Biophysical Fields of Man. Gea Libris, Sofia.

Ignatov, 2010 – *Ignatov, I.* (2010). Which Water is Optimal for the Origin (Generation) of Life? *Euromedica, Hanover.* 34-37.

Ignatov, 2011 – *Ignatov, I.* (2011). Entropy and Time in Living Organisms. *ArchivEuromedica, Hanover, 1st & 2nd Edition.* 74-75.

Ignatov, 2011 – *Ignatov, I.* (2011). Entropy and Time in Living Organisms. *Euromedica, Hanover.* 60-62.

Ignatov, Tsvetkova, 2011 – *Ignatov, I., Tsvetkova, V.* (2011). Water for the Origin of Life and "Informationability" of Water, Kirlian (Electric Images) of Different Types of Water. *Euromedica, Hanover*. 62-65.

Ignatov, Tsvetkova, 2011 – *Mosin, O.V., Ignatov, I.* (2011). Water – Substance of Life, Consciousness and Physical Reality. *Natural Sciences, Moscow*. 17(11): 9-21.

Ignatov et al., 2014 – *Ignatov, I., Karadzhov, S., Atanasov, A., Ivanova, E., Mosin, O.V.* (2014). Electrochemical Aqueous Sodium Chloride Solution (Anolyte and Catholyte) as Types of Water, Mathematical Models, Study of Effects of Anolyte on the Virus of Classical Swine Fever Virus. *Journal of Health, Medicine and Nursing*. 8: 1-28.

Ignatov, Mosin, 2013 – *Ignatov, I., Mosin, O.V.* (2013). Possible Processes for Origin of Life and Living Matter with modeling of Physiological Processes of Bacterium Bacillus Subtilis in Heavy Water as Model System. *Journal of Natural Sciences Research*. 3 (9): 65-76.

Ignatov, Mosin, 2013 – *Ignatov, I., Mosin, O.V.* (2013). Modeling of Possible Processes for Origin of Life and Living Matter in Hot Mineral and Seawater with Deuterium. *Journal of Environment and Earth Science*. 3(14): 103-118.

Ignatov, Mosin, 2013 – *Ignatov, I., Mosin, O.V.* (2013). Structural Mathematical Models Describing Water Clusters. *Journal of Mathematical Theory and Modeling*. 3(11): 72-87.

Ignatov, Mosin, 2015 – *Ignatov, I., Mosin, O.V.* (2015). Origin of Life and Living Matter in Hot Mineral Water. *Advances in Physics Theories and Applications*. 39: 1-22.

Ignatov, 2015 – *Ignatov, I., Mosin, O.V., Gluhchev, G., Karadzhov, S., Miloshev, G., Ivanov, N.* (2015) The Evaluation of Mathematical Model of Interaction of Electrochemically Activated Water Solutions (Anolyte and Catholyte) with Water. *European Reviews of Chemical Research*. 2(4): 72-86.

Ignatov, Pesheva, 2018 – *Ignatov, I., Pesheva, Y.* (2018). Studying of the Factors of Longevity in Smolyan Municipality, Rhodope Mountains, Bulgaria as Area of Oxidant/Antioxidant Balance. *Journal of Natural Sciences Research*. 8(16): 29-42.

Ignatov et al., 2020 – *Ignatov, I., Gluhchev, G., Huether, F.* (2020). Dynamic Nano Clusters of Water on EVODROP Water. *Physical Science International Journal*. 24(7): 47-53.

Ignatov, 2020 – *Ignatov, I.* (2020). Applications of EVODROP Water as Drinking Water of Highest Quality and EVOhygiene Colloidal Silver and Cooper Nano Water. Antibacterial and Antiviral Effects that also Help to Combat SARS-CoV-2. *Scientific Research Center of Medical Biophysics*.

Ignatov et al., 2020 – *Ignatov, I., Valcheva, N., Huether, F.* (2020). Nano and Microbiological Effects of EVODROP Silver and Copper Nanoparticle. *Journal of Materials Science Research and Reviews*. 6(4): 63-71.

Ignatov, Mosin, 2013 – *Ignatov, I., Mosin, O.V.* (2013). Modeling of Possible Processes for Origin of Life and Living Matter in Hot Mineral and Seawater with Deuterium. *Journal of Environment and Earth Science*. 3(14): 103-118.

Ignatov et al., 2014 – *Ignatov, I., Mosin, O. V., Velikov, B., Bauer, E. Tyminski, G.* (2014). Longevity Factors and Mountain Water as Factor. Research in Mountain and Fields Areas in Bulgaria. *Civil and Environmental Research*. 30(4): 51-60.

Ignatov et al., 2021 – *Ignatov, I., Valcheva, N., Mihaylova, S., Dinkov, G.* (2021). Physicochemical and Microbiological Results of Hyperthermal (Hot) Mineral Water in Rupite, Bulgaria as Model System for Origin of Life. *Uttar Pradesh Journal of Zoology*. 41(24): 16-22.

Ignatov, Valcheva, 2021 – *Ignatov, I, Valcheva, N.* (2021). Physiological and Molecular Characteristics of Bacillus Spp. from Warm Mineral Water in Varna, Bulgaria as model system for origin of life. *Uttar Pradesh Journal of Zoology*.

Ignatov et al., 2019 – *Ignatov, I., Mehandjiev, D., Vassileva, P., Voykova, D., Karadzhov, S., Gluhchev, G., Ivanov, N.* (2019). Research of Water Catholyte of Presence of Nascent (Atomic) Hydrogen (H*). Hydrogen and Nascent Hydrogen of the Reactions for Origin of Life in Hot Mineral Water. *European Journal of Medicine*. 7(2): 99-105.

Ignatov et al., 2020 – *Ignatov, I., Gluhchev, G., Karadzhov, G., Yaneva, I., Valcheva, N., Dinkov, G,, Popova, T., Petrova, T., Mehandjiev, D., Akszjonovich, I.* (2020). Dynamic Nano Clusters of Water on Waters Catholyte and Anolyte: Electrolysis with Nano Membranes. *Physical Science International Journal*. 24(1): 46-54.

Tumbarski et al., 2014 – *Tumbarski, T., Valcheva, N., Denkova, Z., Koleva, I.* (2014). Antimicrobial Activity against Some Saprophytic and Pathogenic Microorganisms of Bacillus species Strains Isolated from Natural Sping Waters in Bulgaria. *British Microbiology Research Journal.* 4(12): 1353-1369.

Valcheva, 2020 – *Valcheva, N., Ignatov, I., Huether, F.* (2020). Microbiological Research of the Effects of EVODROP Silver Nanoparticle on Escherichia coli, Enterococci and Coliforms. *Journal of Advances in Microbiology.* 20(11): 22-31.

Valcheva et al., 2013 – *Valcheva, N., Denkova, Z., Denkova, R.* (2013). Physicochemical and microbiological characteristics of spring waters in Haskovo. *Journal of Food and Packaging Science Technique and Technologies.* 2: 21-25.

Valcheva et al., 2014 – *Valcheva, N., Denkova, Z., Nikolova, R., Denkova, R.* (2014) Physiological, Biochemical, and Molecular – Genetic Characterization of Bacterial Strains Isolated From Sping and Healing Waters in Region of Haskovo. *Food, Sciense, Engineering and technologiest, Plovdiv.* LX: 940-946.

Valcheva et al., 2013 – *Valcheva, N., Denkova, Z. Nikolova, Denkova, R.* (2013). Physiological-Biochemical and Molecular – Genetic Characteristics of Bacterial Strains Isolated from Spring and Healing Waters in the Haskovo Region. *N.T. at UCT. Volume LX.*

Valcheva et al., 2014 – *Valcheva, N., Denkova, Z., Denkova, R., Nikolova, R.* (2014). Characterization of bacterial strains isolated from a thermal spring in Pavel Banya, Stara Zagora Region. *N.T. at UCT, Volume LXI.*

Valcheva, 2014 – *Valcheva, N.* (2014) The Microflora of Medicinal and Spring Waters in Haskovo and Stara Zagora Region. Dissertation, University of Food Technology, 1-142.

Valcheva, Ignatov, 2019 – *Valcheva, N., Ignatov, I.* (2019). Physicochemical and Microbiological Characteristics of Thermal Healing Spring Waters in the District of Varna. *Journal of Medicine, Physilogy and Biophysics.* 59: 10-16.

Valcheva et al., 2020 – *Valcheva, N., Ignatov, I., Dinkov, G.* (2020) Microbiological and Physicochemical Research of Thermal Spring and Mountain Spring Waters in the District of Sliven, Bulgaria. *Journal of Advances in Microbiology.* 20(2): 9-17.

Valcheva et al., 2020 – *Valcheva, N., Ignatov, I., Mihaylova, S.* (2020). Physiological and Molecular-genetic Characteristic of Bacteria Strains, Isolated from Mountain Spring and Mineral Waters in Plovdiv Region. *Bulgaria, International Journal of Pathogen Research.* 4(1): 44-55.

Valcheva, Ignatov, 2020 – *Valcheva, N., Ignatov, I.* (2020). Microbiological Research of the Effects of Electromagnetic Fields of the Bacteria Escherichia coli, Enterococci, Coliforms and Clostridium perfringens. *Microbiology Research Journal International.* 30(9): 39-44.

Vassileva et al., 2019 – *Vassileva, P., Voykova, D., Ignatov, I., Karadzhov, S., Gluhchev, S., Ivanov, N., Mehandjiev, D.* (2019). Results from the Research of Water Catholyte with Nascent (Atomic) Hydrogen. *Journal of Medicine, Physiology and Biophysics.* 52: 7-11.

**Standards**

Ordinance №9/2001, Official State Gazette. Is. 30.

Decree № 178/23.07.2004 about the quality of water, intended for drinking purposes.

BDS8451: 1977 – defining of colour according to Rublyovska Scale, determination of smell at 20 °C.

EN ISO 7027 – determination of turbidity.

BDS3424: 1981 – determination ofpH.

BDS3413: 1981 – determination of oxidisability.

BDS3414: 1980 – determination of chlorides.

BDS ISO 6058 – determination of calcium, determination of general hardness.

BDS EN 27888 – determination of electrical conductivity.

VLM – $NH_4$ –№ 1 – determination of ammonium ions.

VLM –$NO_3$ – № 2 – determination of nitrates.

VLM – $NO_2$ –№ 3 – determination of nitrites.

VLM– $SO_4$ –№ 4 – determination of sulphates.

VLM– $PO_4$ –№ 5 – determination of phosphates.

VLM– Fe –№ 6 – determination of iron.

VLM–Mn–№ 7 – determination of manganese.

VLM– F –№ 8 – determination of fluorides.

BDS 7211: 1982 – determination of magnesium.

BDSEN ISO 7899 – 2 –determination of nitrates.

BDSEN ISO 9308 – 1: 2004 – determination of *Escherichia coli*andcoliformbacteria.

BDSEN26461 – 2: 2004 – determination of sulphite reducing anaerobic bacteria *(Clostridiumperfringens)*.

BDSEN ISO 16266 – determination of*Pseudomonas aeruginosa*.

BDSEN ISO 7899 – 2 – determination of eneterococci.

BDS EN ISO 6222: 2002 – determination of total number of aerobic and facultative anaerobic bacteria.

# Origin of Life in Hot Mineral Water. Analyses with Infrared Spectral Methods, pH and ORP. Effects of Hydrogen and Nascent Hydrogen

Ignat Ignatov [a], [*]

[a] Scientific Research Center of Medical Biophysics (SRCMB), Sofia, Bulgaria

**Abstract**

The studies were performed of the composition of water, its temperature, pH and oxidation reduction potential (ORP) value in experiments with modelling of primary hydrosphere and possible conditions for origin of first organic forms of life in hot mineral water in hydrothermal springs and open ponds. Experiments with hot mineral and seawater from Bulgaria by IR-spectroscopy with DNES-method and Thermo Nicolet Avatar 360 Fourier-transform IR were conducted. Cactus juice of *Echinopsis pachanoi* and Jellyfish *Aurelia aurita* from Black Sea were used as model systems. The reactions of condensation and dehydration in alkaline aqueous solutions with pH = 9–11, resulting in synthesis of larger organic molecules as polymers and short polipeptides from separate molecules, were considered and scrutinized. It was shown that hot alkaline mineral water with temperature from +65 °C to +95 °C and pH value from 8.5 to 10 and ORP with negative value is more suitable for the origination of life and living matter than other analyzed water samples. The pH value of seawater on the contrary is limited to the range of 7,5 to 8,4 units. The research was connected with estimation of the common local extremums in hot mineral and sea water, cactus juice and jellyfish.

**Keywords:** origin of life, hot mineral water, hydrothermal conditions, IR-spectroscopy.

## 1. Introduction

Previous biological experiments with $D_2O$ and structural-conformational studies with deuterated molecules, enable to modeling conditions under which the first living forms of life might be evolved (Ignatov, Mosin, 2013). The content of deuterium in hot mineral water may be increased due to the physical chemical processes of the deuterium accumulation. It can be presumed that primary water might contain more deuterium at early stages of evolution of first living structures, and deuterium was distributed non-uniformly in the hydrosphere and atmosphere (Ignatov, Mosin, 2012). The primary reductive atmosphere of the Earth consisted basically of gas mixture CO, $H_2$, $N_2$, $NH_3$, $CH_4$, lacked $O_2$–$O_3$ layer protecting the Earth surface from rigid short-wave solar radiation carrying huge energy capable to cause radiolysis and photolysis of water.

The point regards the influence of temperature on the processes in living matter. Recent studies have shown that the most favorable for the origin of life and living matter seem to be hot alkaline mineral waters interacting with $CaCO_3$ (Ignatov, 2010; Ignatov, Mosin, 2013). According to the law for conservation of energy the process of self-organization of primary organic forms in water solutions may be supported by thermal energy of magma, volcanic activity and solar radiation. According to J. Szostak, the accumulation of organic compounds in open lakes is more

---

[*] Corresponding author
E-mail addresses: mbioph@abv.bg (I. Ignatov)

possible compared to the ocean (Szostak, 2011). Probably the life has begun near a hydrothermal vent: an underwater spout of hot water. Geothermal activity gives more opportunities for the origination of life. In 2009 A. Mulkidjanian and M. Galperin demonstrate that the cell cytoplasm contains potassium (K), zinc (Zn), manganese (Mn) and phosphate ions (P), which are not particularly widespread in the sea aquatorium (Mulkidjanian, Galperin, 2009). Colín-García and co-authors also summarize a set of experiments proposed to test the role of hydrothermal vents in prebiotic synthesis (Colín-García et al., 2016). B. Damer and D. Deamer have come to the conclusion that cell membranes cannot be formed in salty seawater. Before the continents formed, the only dry land on Earth would be volcanic islands, where rainwater would form ponds where lipids could form the first stages towards cell membranes. Only when true cells had evolved they gradually would adapt to saltier environments and enter the ocean (Damer, Deamer, 2015). J. Trevors and G. Pollack were proposed that the first cells on the Earth assembled in a hydrogel environment (Trevors, Pollack, 2005). Gel environments are capable of retaining water, oily hydrocarbons, solutes, and gas bubbles, and are capable of carrying out many functions, even in the absence of a membrane. Hydrocarbons are an organic compounds consisting entirely of hydrogen (H) and carbon (C). The analyses show the possible scenario of the syntheses of periodically molecules of life (Colón Santos, 2019). The data presented in this paper show that the origination of living matter most probably occurred in hot mineral water. This occurred in hydrothermal springs and ponds with hot mineral water. There had been possible also in hydrothermal vents in seawater with hot mineral water. An indisputable proof of this is the presence of stromatolites fossils. They lived in warm and hot water in zones of volcanic activity, which could be heated by magma and seem to be more stable than other first sea organisms (Ignatov, 2012).

The purpose of the research was studying the conditions of primary hydrosphere (temperature, pH, ORP, isotopic composition) for possible processes for origin of life and living matter in hot mineral water. There was studied primary atmosphere and interaction with hydrosphere and with effects of gas discharge. Various samples of water from Bulgaria were studied within the frames of the research.

The aim of the research and analyses was to study the parameters of hot mineral water from Rupite, Bulgaria with calcium and hydrocarbonate ions as model system for origin of life. In 2020 were performed studies of hot mineral water from Rupite (Ignatov et al., 2021) and warm mineral water from Varna (Ignatov, Valcheva, 2021). The researches were with microbiological parameters of genus Bacillus and its evolutionary development.

### 2. Material and methods
### 2.1. Objects of Studying
The research by the IR-spectrometry with DNES-method (Antonov, 1995; Antonov, Ignatov, 1998) was carried out with samples of water taken from various water sources:

1 – mineral water (Rupite, Bulgaria);

2 – seawater (Varna, Bulgaria);

Sediments from hot mineral spring and pond in Rupite, Bulgaria and sea salt from Black Sea were studied using the Thermo Nicolet Avatar 360 Fourier-transform IR;

Cactus juice of *Echinopsis pachanoi* and Jellyfish *Aurelia aurita* (Varna, Bulgaria, Black Sea) were used as two model systems which were both investigated by the IR-spectrometry with DNES method.

### 2.2. IR-Spectroscopy
IR-spectra of water samples were registered on Thermo Nicolet Avatar 360 Fourier-transform IR (K. Chakarova) and Differential Non-equilibrium Spectrum (DNES).

### 2.3. pH indicator and oxidation reduction potential (ORP)
The research of pH and ORP with Hanna instruments was performed.

### 3. Results and discussion
Research of various samples of mineral water from mineral springs and seawater from Bulgaria was carried out. The hot mineral spring and ponds of Rupite are located in eastern foot of the extinct volcano Kozhuh.

**Table 1.** Results with DNES spectral method and Thermo Nicolet Avatar 360 Fourier-transform IR of cactus juice, jelly fish, sea water and salt, sea water and salt, mineral water and sediments from Rupite, Bulgaria

| -E (eV); λ (μm); k (cm⁻¹) DNES-method | -E (eV); λ (μm); k (cm⁻¹) DNES-method | λ (μm); k (cm⁻¹) Thermo Nicolet Avatar 360 Fourier-transform IR | -E (eV); λ (μm); k (cm⁻¹) DNES-method | λ (μm); k (cm⁻¹) Thermo Nicolet Avatar 360 Fourier-transform IR | -E (eV); λ (μm); k (cm⁻¹) DNES-method |
|---|---|---|---|---|---|
| Cactus juice | Mineral water Rupite (Bulgaria) | Mineral water Rupite (Bulgaria) | Sea Water Black Sea | Sea salt Black Sea | Jelly fish Black Sea |
| 0.1112 (**11.15**; 897) | 0.1112 (**11.15**; 897) | (**11.44**; 875) | | | |
| 0.1187 (**10.45**; 957) | 0.1187 (**10.45**; 957) | (**10.95**; 913) | | | 0.1200; (**10.33**; 968) |
| 0.1262 (**9.82**;1018) | 0.1262 (**9.82**; 1018) | | | | |
| 0.1287 (**9.63**; 1038) | 0.1287 (**9.63**; 1038) | (**9.78**; 1031) | | | |
| 0.1362 (9.10;1099) | – | (**9.08**;1101) | 0.1362 (**9.10**;1099) | | (0.1375; **9.02**; 1109) |
| 0.1387 | 0.1387 (**8.95**; 1117) | – | | (**8.93**;1120) | |

Note:
*The function of the distribution of energies Δf was measured in reciprocal electron volts (eV⁻¹). It is shown at which values of the spectrum -E (eV) the biggest local maximums of this function are observed; λ – wave length; κ – wave number.

For this DNES method was employed for research of cactus juice *Echinopsis pachanoi* (Table 1). The cactus was selected as a model system because this plant contains approximately 90 % of water. The closest to the spectrum of cactus juice was the spectrum of mineral water contacting with $Ca^{2+}$ and $HCO_3^-$ ions from Rupite, Bulgaria (Table 1).

DNES-spectra of cactus juice and mineral water from Rupite, Bulgaria with $HCO_3^-$ (1320–1488 mg/L), $Ca^{2+}$ (29–36 mg/L) t=76 °C (source) and t=52-54 °C (open ponds depending the season) have magnitudes of local extremums at −0.1112 (11.15); -0.1187 (10.45); -0.1262 (9.83); -0.1287 (9.64) and −0.1387 eV (9.85 μm). Similar local extremum in the DNES-spectrum between cactus juice and seawater were detected at -0,1362 eV (9.10 μm).

Common extremums in the IR-spectrum between cactus juice (DNES method) and minerals from the sediments (Thermo Nicolet Avatar 360 Fourier-transform IR) were detected at 11.44; 10.95; 9.78; 9.08; μm. Similar local extremum between cactus juice and sea salt was detected at 8.93 μm.

Study of the local extremums in DNES spectrum of jellyfish from Black Sea was performed (Table 1). There are two local extremums at 9.02 and 10.33 μm. The local extremum at 9.02 μm corresponds to the local extremums in sea salt (8.93 μm).

The local extremums of sediments from hot mineral spring in Rupite, Bulgaria were studied with Thermo Nicolet Avatar 360 Fourier-transform IR (Figure 2).
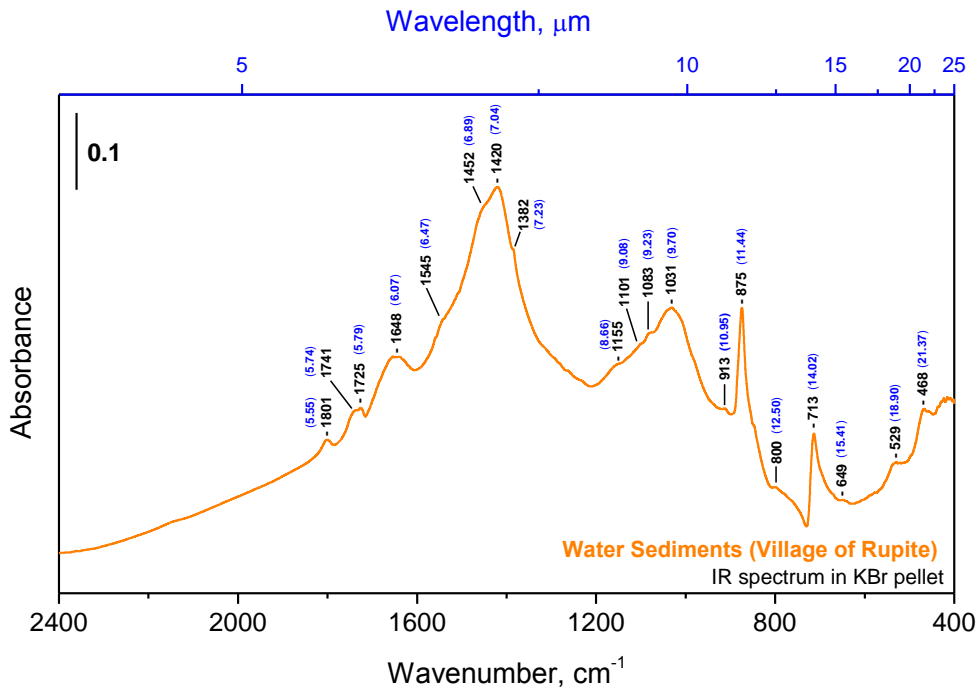
**Fig. 2.** IR-spectrum of water obtained from Rupite Village (Bulgaria)

The results with DNES method indicated that jellyfish *Aurelia aurita* had local exremums at 9.02 and 10.33 μm in IR-spectra (Table 1). Before measurements the jellyfish was kept in seawater for several days. For comparison seawater has a local extremum at 9.10 μm with DNES method and Sea salt 8.93 μm with Nicolet Avatar 360 Fourier-transform IR (Figure 3). Jellyfish contains approximately 97 (w/w) % of water and is the most unstable living organism compared to those ones that form stromatolites. The explanation for this is the smaller concentration of salts and, therefore, the smaller number of local extremums in the IR-spectrum in relation to seawater.
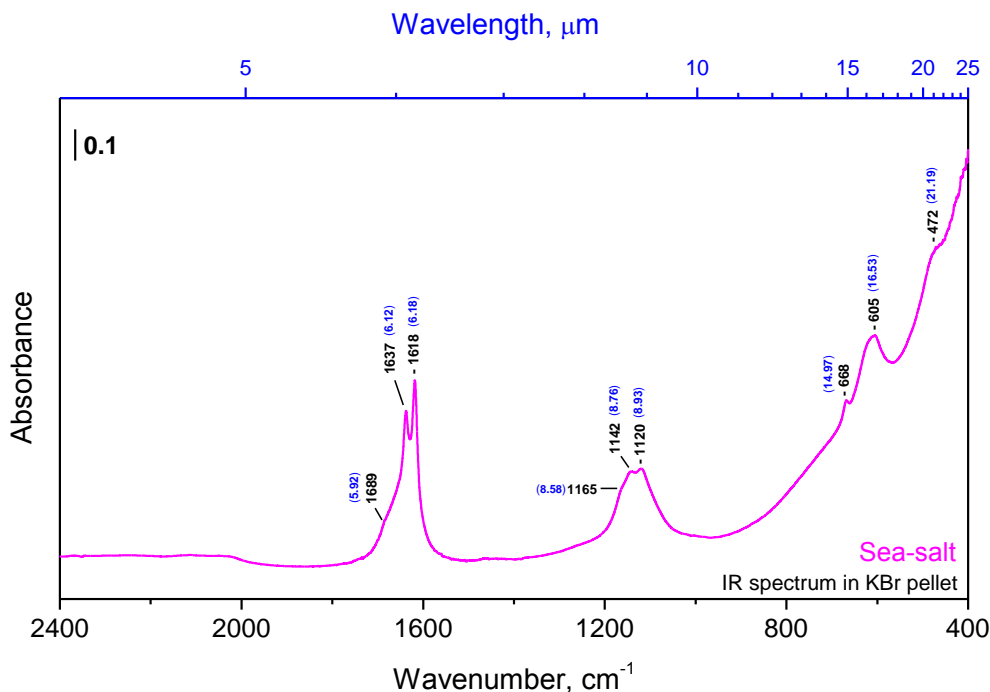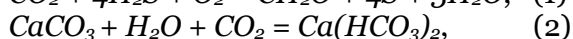


**Fig. 3.** IR-spectrum of seasalt obtained from Varna (Bulgaria)

Such a character of IR-spectrums and distribution of local extremums may prove that hot mineral alkaline water is preferable for origin and maintenance of life compared to other types of water analyzed by DNES and Nicolet Avatar 360 Fourier-transform IR. Thus, in hot mineral waters

the local extremums in the IR-spectrums are more manifested compared to the local extremums obtained in IR-spectrum of the same water at a lower temperature (Ignatov, 2013). The difference in the local extremums in the interval from +20 $^{o}$C to +95 $^{o}$C at each 5 $^{o}$C step is significant at p < 0.05 according to Student's t-criterion. These data indicate that the origination of life and living matter depends on the structure and physical chemical properties of water, as well as its temperature. The IR-spectrum of cactus juice is the closest to the IR- and DNES-spectrum of water, which contains bicarbonates and calcium ions typical for the formation of stromatolites. For this reason cactus juice was applied as a model system. The local extremums in IR-spectra of alkaline mineral water interacting with $CaCO_3$ and then seawater are the. The most closed closest to the local extremums in IR-spectrum of cactus juice.

In connection with these data the following reactions participating with $CaCO_3$ in aqueous solutions are important:

$$CO_2 + 4H_2S + O_2 = CH_2O + 4S + 3H_2O, \quad (1)$$
$$CaCO_3 + H_2O + CO_2 = Ca(HCO_3)_2, \quad (2)$$
$$CO_2 + OH^- = HCO_3^- \quad (3)$$
$$2HCO_3^- + Ca^{2+} = CaCO_3 + CO_2 + H_2O \quad (4)$$

The equation (1) shows how some chemosynthetic bacteria use energy from the oxidation of $H_2S$ and $CO_2$ to S and formaldehyde ($CH_2O$). The equation (2) is related to one of the most common processes in nature: in the presence of $H_2O$ and $CO_2$, $CaCO_3$ transforms into $Ca(HCO_3)_2$. In the presence of hydroxyl $OH^-$ ions, $CO_2$ transforms into $HCO_3^-$ (equation (3)). Equation (4) is valid for the process of formation of the stromatolites – the dolomite layered acretionary structures formed in shallow seawater by colonies of cyanobacteria. In 2010 D. Ward described fossilized stromatolites in the Glacier National Park (USA) (Schirber, 2010). Stromatolites aged 3.5 billion years had lived in warm and hot water in zones of volcanic activity, which could be heated by magma. This suggests that the first living forms evidently evolved in hot geysers (Pons et al., 2011). It is known that water in geysers is rich in carbonates, while the temperature is ranged from +60 to +100 $^{o}$C and more than +100 $^{o}$C. In 2011 a team of Japanese scientists under the leadership of T. Sugawara showed that life originated in warm or, more likely, hot water (Kurihara et al., 2011). DNA and synthetic enzymes created proto cells from aqueous solution of organic molecules. For this the initial solution was heated to a temperature close to water's boiling point +95 $^{o}$C. Then its temperature was lowered to +65 $^{o}$C with formation of proto cells with primitive membrane. This laboratory experiment is an excellent confirmation of the possibility that life originated in hot water.

The above-mentioned data can predict a possible transition from synthesis of small organic molecules under high temperatures to more complex organic molecules as proteins. There are reactions of condensation-dehydration of amino acids into separate blocks of peptides that occur under alkaline conditions, with pH = 9–11.

A research is conducted of Oxidation Reduction Potential (ORP) of hot mineral water from Rupite, Bulgaria. With temperature increase ORP gets reduced with (-70 mV) from 50 to 25° C (Table 2). The measured pH is 7.70. The change of ORP shows that in hot mineral water are released electrons in alkaline medium.

**Table 2.** Results of temperature (°C) and Oxidation Reduction Potential (ORP) of mineral water from Rupite, Bulgaria

| Temperature (° C) | Oxidation Reduction Potential (ORP) (mV) |
|---|---|
| 25 | 57 |
| 30 | 45 |
| 35 | 37 |
| 40 | 30 |
| 45 | 18 |
| 50 | -13 |

When reviewing the processes of life origin it is necessary to consider the composition of primary atmosphere 3.5 billion years ago. It contains $H_2$, $N_2$, $CO_2$, CO. With the temperature rise of

the water and boiling in the modern atmosphere, the bubbles contain oxygen and it gets acidified. The author suggests that the bubbles in the water in contact with the ancient atmosphere contain hydrogen, and the water gets more alkaline. Also ORP decreases and may result in negative values. An experiment is conducted with saturation of water from Rupite with hydrogen. The achieved average result is (-215 mV) with temperature 50°C. The difference is (-215 mV)- (-13 mV)= (-202 mV). This indicates that in the ancient atmosphere were gained more electrons in the water. In such a way are achieved more hydroxyl groups ($OH^-$) and bicarbonate ions ($HCO_3^-$).

The interaction with calcium ions ($Ca^{2+}$) during exchange of electric charges as per formulae makes the processes for structuring of stromatolites by formulae (1) and (2) more active.

$$CO_2 + OH^- = HCO_3^- \qquad (3)$$
$$2\ HCO_3^- + Ca^{2+} = CaCO_3 + CO_2 + H_2O \quad (4)$$
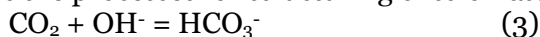
The following reaction (5) is valid in electrolysis. In the ancient atmosphere and hydrosphere there was increased gas discharge.

$$2H_2O + 2\ e^- = H_2 + 2OH^- \qquad (5)$$

The same reaction contributed for the formation of stromatolites. Nowadays it is observed in elecrolyzer devices for waters catholyte and anolyte. In the ancient hydrosphere and land the charge had been negative and in the atmosphere positive. The conditions had been optimal for "nature" electrolysis. In these direction had been the experiments of Miller (Miller, 1953).

The reaction (4) is possible to structure nascent hydrogen $H^*$ (Mehandjiev et al., 2019).

$$H_2O + e^- \rightarrow H^* + OH^-, \qquad (6)$$
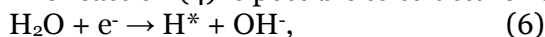
The reaction (5) released in the gaseous form after recombination is formed:

$$H^* + H^* \rightarrow H_2 \qquad (7)$$

The nascent hydrogen is very active for chemical reactions in primary hydrosphere for origin of life and there isadditional $H_2$ in primary hydrosphere with dissolving from atmosphere.

The allocation of $H_2O$ molecule when a peptide chain is formed is important factor in reaction of condensation of two amino acid molecules into dipeptide. As reaction of polycondensation of amino acids is accompanied by dehydration, the $H_2O$ removal from reaction mixture speeds up the reaction rate. This testifies that formation of early organic forms may have occured nearby active volcanoes, because at early periods of geological history volcanic activity occurred more actively than during subsequent geological times. However, dehydratation accompanies not only amino acid polymerization, but also association of other small blocks into larger organic molecules, and also polymerization of nucleotides into nucleic acids. Such association is connected with the reaction of condensation, at which from one block a proton is removed, and from another – a hydroxyl group with the formation of $H_2O$ molecule (Ignatov, Mosin, 2012)

The results with ORP show that free electrons in water support for amino acid polymerization and small blocks into larger organic molecules (Ignatov, 2019).

In 1969 the possibility of existence of condensation-dehydration reactions under conditions of primary hydrosphere was proven by M. Calvin (Calvin, 1969). From most chemical substances hydrocyanic acid (HCN) and its derivatives – cyanoamid ($CH_2N_2$) and dicyanoamid ($HN(CN)_2$) possess dehydration ability and the ability to catalyze the process of linkage of $H_2O$ from primary hydrosphere (Mathews, Moser, 1968). The presence of HCN in primary hydrosphere was proven by S. Miller's early experiments (Miller, 1953). Chemical reactions with HCN and its derivatives are complex with a chemical point of view; in the presence of HCN, $CH_2N_2$ and $HN(CN)_2$ the condensation of separate blocks of amino acids accompanied by dehydration can proceed at normal temperatures in strongly diluted $H_2O$-solutions. These reactions show the results of synthesis from separate smaller molecules to larger organic molecules of polymers, e.g. proteins, polycarboxydrates, lipids, and ribonucleic acids.

Furthermore, polycondensation reactions catalyzed by HCN and its derivatives depend on acidity of water solutions in which they proceed (Abelson, 1966). In acid aqueous solutions with pH = 4–6 these reactions do not occur, whereas alkaline conditions with pH = 9–11 promote their course. There has not been unequivocal opinion, whether primary water was alkaline, but it is probable that such pH value possessed mineral waters adjoining with basalts, i.e. these reactions could occur at the contact of water with basalt rocks, that testifies this hypothesis (Ignatov, Mosin, 2012).

It should be noted, that geothermal sources might be used for synthesis of various organic molecules. Thus, amino acids were detected in solutions of formaldehyde $CH_2O$ with

hydroxylamine NH$_2$OH, formaldehyde with hydrazine (N$_2$H$_4$) in water solutions with HCN, after heating of a reactionary mixture to +95 ℃ (Harada, Fox, 1964). In model experiments reaction products were polymerized into peptide chains that are the important stage towards inorganic synthesis of protein. Purines and pyrimidines were formed in a reactionary mixture of water solution with a HCN–NH$_3$. In other experiments amino acid mixtures were subjected to influence of temperatures from +60 ℃ up to +170 ℃ with formation of short protein-like molecules resembling early evolutionary forms of proteins subsequently designated as thermal proteinoids (Ignatov, Mosin, 2012). They consisted of 18 amino acids usually occurring in protein hydrolyzates. The synthesized proteinoids are similar to natural proteins on a number of other important properties, e. g. on linkage by nucleobases and ability to cause the reactions similar to those catalyzed by enzymes in living organisms as decarboxylation, amination, deamination, and oxidoreduction. Proteinoids are capable to catalytically decompose glucose (Fox, Krampitz, 1964) and to have an effect similar to the action of α-melanocyte-stimulating hormone (Fox, Wang, 1968). The best results on polycondensation were achieved with the mixes of amino acids containing aspartic and glutamic acids, which are essential amino acids occurring in all modern living organisms.

In natural conditions water was heated by the magma. The structure formed from heated water was evidently a result of self-organization. Living organisms are complex self-organizing systems. They are open because they constantly exchange substances and energy with the environment and change the entropy (Ignatov, 2011). The changes in the open systems are relatively stable in time. The stable correlation between components in an open system is called a dissipative structure. According to I. Prigozhin, the formation of dissipative structures and the elaboration to living cells is related to changes in entropy (Nikolis, Prigozhin, 1979).

The initial stage of evolution, apparently, was connected with formation of the mixtures of amino acids and nitrogenous substances – analogues of nucleic acids at high temperature. Such synthesis is possible in aqueous solutions under thermal conditions in the presence of H$_3$PO$_4$. The next stage is polycondensation of amino acids into thermal proteinoids at temperatures 65−95 ℃. After that membrane like structures were formed in a mix of proteinoids in hot water solutions. In 2011 T. Sugawara (Japan) created membrane like proto cells from aqueous solution of organic molecules, DNA and synthetic enzymes under temperature close to water's boiling point +95 ℃ (Sugawara, 2011).

### 4. Conclusion
The data obtained testify that origination of life and living matter depends on physical-chemical properties of water and external factors – temperatures, pH, ORP, electric discharges and isotopic composition. Hot mineral alkaline water interacting with CaCO$_3$ is closest to these conditions. Next in line with regard to quality is seawater. For chemical reaction of dehydration-condensation to occur in hot mineral water, water is required to be alkaline with pH range 9–11 and negative ORP. In warm and hot mineral waters the local extremums in IR-spectrums from 8 to 14 μm were more expressed in comparison with the local extremums measured in the same water samples with lower temperature. The new achievement is connected with chemical composition of ancient atmosphere and alkalization of the water from the hydrogen.

The research for origin of life and living matter in hot mineral water in mineral springs and open ponds (Ignatov, 2010; Szostak, 2011; Damer, Deamer, 2015) and in hydrothermal vents in the ocean (Mulkidjanian, Galperin, 2009) give the possibilities for life at the surface of the moons of the planets in Solar System. According to the law for conservation of energy the process of self-organization of primary organic forms in water solutions may be supported by thermal energy of magma (Ignatov, 2010). The candidates are – Europa (moon of Jupiter), Titan and Enceladus (moons of Saturn).

### 5. Acknowledgements

### References
Abdullah et al., 2012 – *Abdullah, A.M., Abdelsalam, E., Abdullah, B., Khaled, A.* (2012).

Antioxidant Effects of Zamzam Water in Normal Rats and Those Under Induced-oxidant Stress, *Journal of Medicinal Plants Research*. 6(42): 5507-5512.

Abelson, 1966 – *Abelson, P.* (1966). Chemical Events on the "Primitive" Earth. *Proc. Natl. Acad. Sci. U.S.* 55: 1365-1372.

Antonov, 1995 – *Antonov, A.* (1995). Research of Nonequilibrium Processes in the Area of Allocated Systems, Diss. Thesis Doctor of Physical Sciences, 1-255.

Calvin, 1969 – *Calvin, M.* (1969). Chemical evolution. *Oxford: Clarendon*. 278.

Colin et al., 2016 – *Colin, G. et al.* (2016). Hydrothermal Vents and Prebiotic Chemistry: a Review. *Boletín de la Sociedad Geológica Mexicana*. 1-22.

Colon Santos, 2019 – *Colon Santos, S.M.* (2019). Exploring the Untargeted Synthesis of Prebiotically-plausible Molecules. *PhD Thesis, University of Glasgow*. 1-231.

Damer, Deamer, 2015 – *Damer, B., Deamer, D.* (2015). Coupled Phases and Combinatorial Selection in Fluctuating Hydrothermal Pools: A Scenario to Guide Experimental Approaches to the Origin of Cellular Life. *Life*. 5(1): 872-887.

Fox, Krampitz, 1964 – *Fox, S.W., Krampitz, G.* (1964). Catalytic Decomposition of Glucose in Aqueous Solution by Thermal Proteinoids. *Nature*. 203: 1362-1364.

Fox, Wang, 1968 – *Fox, S.W., Wang, C.T.* (1968). Melanocytestimulating hormone: Activity in thermal polymers of alpha-ammo acids. *Science*. 160: 547-548.

Harada, Fox, 1964 - *Harada, I., Fox, S.W.* (1964). Thermal Synthesis of Natural Ammo-acids from a Postulated Primitive Terrestrial Atmosphere. *Nature*. 201: 335-336.

Ignatov et al., 1998 – *Ignatov, I., Antonov, A., Galabova, T.* (1998). Medical Biophysics – Biophysical Fields of Man. *Gea Libris, Sofia*.

Ignatov, 2010 – *Ignatov, I.* (2010). Which Water is Optimal for the Origin (Generation) of Life? *Euromedica, Hanover*. 34-37.

Ignatov, 2011 – *Ignatov, I.* (2011). Entropy and Time in Living Organisms. *ArchivEuromedica, Hanover, 1st & 2nd Edition*. 74-75.

Ignatov, 2011 – *Ignatov, I.* (2011). Entropy and Time in Living Organisms. *Euromedica, Hanover*. 60-62.

Ignatov, Tsvetkova, 2011 – *Ignatov, I., Tsvetkova, V.* (2011). Water for the Origin of Life and "Informationability" of Water, Kirlian (Electric Images) of Different Types of Water. *Euromedica, Hanover*. 62-65.

Ignatov, Tsvetkova, 2011 – *Mosin, O.V., Ignatov, I.* (2011). Water – Substance of Life, Consciousness and Physical Reality. *Natural Sciences, Moscow*. 17 (11): 9-21.

Ignatov, Mosin, 2012 – *Ignatov, I., Mosin, O.V.* (2012). Hot Mineral Water with a High Deuterium Content in the Process of the Origin of Life and Living matter. *Everything about Water, Moscow*. 1-26.

Ignatov, Mosin, 2012 – *Ignatov, I., Mosin, O.V.* (2012). Hot Mineral Water with Deuterium Molecules for the Origin of Life and Living Matter. *Congress Science, Information, Consciousness, Saint-Petersburg Technical University*. 137-149.

Ignatov, 2012 – *Ignatov, I.* (2012). Origin of Life and Living Matter in Hot Mineral Water, *Conference on the Physics, Chemistry and Biology of Water, Vermont Photonics, USA*.

Ignatov, Mosin, 2012 – *Ignatov, I., Mosin, O.V.* (2012). Isotopic Composition of Water and its Temperature in Modeling of Primordial Hydrosphere Experiments, *Euro-Eco, Hanover*. 62.

Ignatov, Mosin, 2012 – *Ignatov, I., Mosin, O.V.* (2012). Isotopic Composition of Water and its Temperature in Modeling primordial Hydrosphere Experiments, *VII Int. Conference Future Studies in Science and Technology, Veterinary Biological Science, Prague*. 15: 41-49.

Ignatov, Mosin, 2013 – *Ignatov, I., Mosin, O.V.* (2013). Ideas about the Origin of Life in the Light of the Study of the Properties of the Natural Water. *Chemistry, Moscow*. 10: 3-9.

Ignatov et al., 2014 – *Ignatov, I., Karadzhov, S., Atanasov, A., Ivanova, E., Mosin, O.V.* (2014). Electrochemical Aqueous Sodium Chloride Solution (Anolyte and Catholyte) as Types of Water, Mathematical Models, Study of Effects of Anolyte on the Virus of Classical Swine Fever Virus. *Journal of Health, Medicine and Nursing*. 8: 1-28.

Ignatov, Mosin, 2013 – *Ignatov, I., Mosin, O.V.* (2013). Origin of Life in Hot Mineral Water with Deuteriun. *Everything about Water, Moscow*. 1-15.

Ignatov, Mosin, 2013 – *Ignatov, I., Mosin, O.V.* (2013). Isotopic Composition of Water and its Temperature in Modeling of Primordial Hydrosphere Experiments for Origin of Life and Living Matter. *Science Review, Moscow.* 1: 17-27.

Ignatov, Mosin, 2013 – *Ignatov, I., Mosin, O.V.* (2013). Isotopic Composition of Water and its Temperature in Modeling of Primordial Hydrosphere Experiments for Origin of Life and Living Matter. *Acknowledge, Moscow.* 14(1): 1-16.

Ignatov, Mosin, 2013 – *Ignatov, I., Mosin, O.V.* (2013). Origin of Life and Living Matter in Hot Mineral Water. *Acknowledge, Moscow.* 15(2): 1-19.

Ignatov, Mosin, 2013 – *Ignatov, I., Mosin, O.V.* (2013). Structure of Water for Origin of Life and Living Matter. *Acknowledge, Moscow.* 15(2): 1-16.

Ignatov, Mosin, 2013 – *Ignatov, I., Mosin, O.V.* (2013). Isotopic Composition of Water and Origin of Life. *School Biology, Moscow.* 3: 5-16.

Ignatov, Mosin, 2013 – *Ignatov, I., Mosin, O.V.* (2013). Isotopic Composition of Water and its Temperature in the Process of Evolutional Development of Life and Living Matter. *Astrahan Newspaper of Ecological Development, Astrahan.* 1, 113-127.

Ignatov, Mosin, 2013 – *Ignatov, I., Mosin, O.V.* (2013). Possible Processes for Origin of Life and Living Matter with modeling of Physiological Processes of Bacterium Bacillus Subtilis in Heavy Water as Model System. *Journal of Natural Sciences Research.* 3(9): 65-76.

Ignatov, Mosin, 2013 – *Ignatov, I., Mosin, O.V.* (2013). Biological Effect of Deuterium on Prokaryotic and Eukaryotic Cells. *Astrahan Newspaper of Ecological Development.* 3: 124-138.

Ignatov, Mosin, 2013 – *Ignatov, I., Mosin, O.V.* (2013). Modeling of Possible Processes for Origin of Life and Living Matter in Hot Mineral and Seawater with Deuterium. *Journal of Environment and Earth Science.* 3(14): 103-118.

Ignatov, Mosin, 2013 – *Ignatov, I., Mosin, O.V.* (2013). Isotopic Composition of Water and its Temperature in Modeling of Primordial Hydrosphere Experiments for Origin of Life and Living Matter. *Consciousness and Physical Reality, Natural Science, Moscow.* 18(4): 26-32.

Ignatov, Mosin, 2014 – *Ignatov, I., Mosin, O.V.* (2014). Modeling of Possible Processes for Origin of Life and Living Matter in Hot Mineral Water. Research of Physiological Processes of Bacterium Bacillus Subtilis in Hot Heavy Water. *Journal of Medicine, Physiology and Biophysics.* 2: 53-70.

Ignatov, Mosin, 2014 – *Ignatov, I., Mosin, O.V.* (2014). Modeling of Possible Conditions For Origin of First Organic Forms in Hot Mineral Water. *Journal of Medicine, Physiology and Biophysics.* 3: 1-14.

Ignatov, Mosin, 2014 – *Ignatov, I., Mosin, O.V.* (2014). Modeling of Possible Processes for Origin of Life and Living Matter in Sea and Hot Mineral Water. Process of Formation of Stromatolites. *Journal of Medicine, Physiology and Biophysics.* 5: 23-46.

Ignatov, Mosin, 2014 – *Ignatov, I., Mosin, O.V.* (2014). Hot Mineral Water with More Deuterium for Origin of Live and Living Matter. Process of Formation of Stromatolites. *Journal of Health, Medicine and Nursing.* 6: 1-24.

Ignatov, Mosin, 2014 – *Ignatov, I., Mosin, O.V.* (2014). Origin of Life and Living Matter in Primary Atmosphere and Hydrosphere. Modeling of Non-equilibrium Electric Gas Discharge Conditions. *Journal of Health, Medicine and Nursing.* 6: 25-49.

Ignatov, Mosin, 2014 – *Ignatov, I., Mosin, O.V.* (2014). Modeling of Conditions in Primary Hydrosphere in the Process of Origination of Organic Forms of Life in Hot Mineral Water. N*anoengineering, Moscow.* 6: 37-46.

Ignatov, Mosin, 2015 – *Ignatov, I., Mosin, O.V.* (2015). Origin of Life and Living Matter in Hot Mineral Water. *Advances in Physics Theories and Applications.* 39: 1-22.

Ignatov et al., 2015 – *Ignatov, I., Mosin, O.V., Gluhchev, G., Karadzhov, S., Miloshev, G., Ivanov, N.* (2015). The Evaluation of Mathematical Model of Interaction of Electrochemically Activated Water Solutions (Anolyte and Catholyte) with Water. *European Reviews of Chemical Research.* 2(4): 72-86.

Ignatov, Mosin, 2015 – *Ignatov, I., Mosin, O.V.* (2015). Non-equilibrium Gas Discharge Conditions for Origin of Life and Living Matter. Experiments of Miller. Modeling of the Conditions with Gas Coronal Discharge Simulating Primary Atmosphere. *Journal of Medicine, Physiology and Biophysics.* 9: 27-50.

Ignatov, Mosin, 2015 – *Ignatov, I., Mosin, O.V.* (2015). Hydrothermal Conditions for Origin of Life and Living Matter. *Journal of Health, Medicine and Nursing*. 10:1-33.

Ignatov, Mosin, 2015 – *Ignatov, I. Mosin, O.V.* (2015). Studying the Hydrological Conditions for Origin of First Organic Forms of Life in Hot Mineral Water with HDO. *Journal of Medicine, Physiology and Biophysics*. 15: 20-41.

Ignatov, Mosin, 2015 – *Ignatov, I., Mosin, O.V.* (2015). S. Miller's Experiments in Modelling of Non-Equilibrium Conditions with Gas Electric Discharge Simulating Primary Atmosphere. *Journal of Medicine, Physiology and Biophysics*. 15: 61-76.

Ignatov, Mosin, 2015 – *Ignatov, I., Mosin, O.V.* (2015). Possible Processes for Origin of First Chemoheterotrophic Microorganisms with Modeling of Physiological Processes of Bacterium Bacillus Subtilis as a Model System in 2H2O. *Journal of Medicine, Physiology and Biophysics*. 17: 53-75.

Ignatov, Mosin, 2015 – *Ignatov, I., Mosin, O.V.* (2015). Studying the Properties of Hot Mineral Water to Sustain the Organic Forms of Life by IR, NES and DNES Methods. *Journal of Medicine, Physiology and Biophysics*. 18: 1-14.

Ignatov, Mosin, 2015 – *Ignatov, I., Mosin, O.V.* (2015). Possible Processes for Origin of First Chemoheterotrophic Microorganisms with Modeling of Physiological Processes of Bacterium Bacillus subtilis as a Model System in 2H2O. *European Journal of Molecular Biotechnology*. 9 (3): 131-155.

Ignatov, Mosin, 2016 – *Ignatov, I., Mosin, O.V.* (2016). Isotopic Composition, the Temperature and pH Value of Water in Experiments with Prognosis of Primary Hydrosphere and Possible Conditions for Origin of First Organic Forms in Hot Mineral Water with HDO. *Journal of Medicine, Physiology and Biophysics*. 24: 18-41.

Ignatov, Mosin, 2016 – *Ignatov, I., Mosin, O.V.* (2016). The Reactions of Condensation–Dehydration Occurring in Aqueous Alkaline Solutions at pH = 9–11 and t = 65–95 °C in the Process of Modeling of Primary Hydrosphere. *Journal of Medicine, Physiology and Biophysics*. 24: 42-55.

Ignatov, Mosin, 2016 – *Ignatov, I., Mosin, O.V.* (2016). Studying the Process of Formation of Precambrian Period Limestone Dolomite Fossils of Stromatolites in Hot Mineral Water Interacting with $CaCO_3$. *Journal of Medicine, Physiology and Biophysics*. 25: 29-44.

Ignatov, Mosin, 2016 – *Ignatov, I., Mosin, O.V.* (2016). The Formation of Thermal Proteinoids in Hot Water. *Journal of Medicine, Physiology and Biophysics*. 26: 15-27.

Ignatov, Mosin, 2016 – *Ignatov, I., Mosin, O.V.* (2016). Deuterium, Heavy Water and Origin of Life. *LAP LAMBERT Academic Publishing*. 1-500.

Ignatov, Mosin, 2016 – *Ignatov, I., Mosin, O.V.* (2016). Water and Origin of Life. *Altaspera Publishing & Literary Agency Inc*. 1-616.

Ignatov, Mosin, 2016 – *Ignatov, I., Mosin, O.V.* (2016). Can the First Organic Forms Of Life Originate in Hot Mineral Water with HDO? *Russian Journal of Biological Research*. (7)1: 4-19.

Ignatov, Mosin, 2016 – *Ignatov, I., Mosin, O.V.* (2016). Water and Origin of Life: Collection of Scientific Publications. *Moscow, Berlin, Direct Media*, pp. 1-658.

Ignatov et al., 2021 – *Ignatov, I., Valcheva, N., Mihaylova, S., Dinkov, G.* (2021). Physicochemical and Microbiological Results of Hyperthermal (Hot) Mineral Water in Rupite, Bulgaria as Model System for Origin of Life. *Uttar Pradesh Journal of Zoology*. 41(24): 16-22.

Ignatov, Valcheva, 2021 – *Ignatov, I, Valcheva, N.* (2021). Physiological and Molecular Characteristics of Bacillus Spp. from Warm Mineral Water in Varna, Bulgaria as model system for origin of life. *Uttar Pradesh Journal of Zoology*.

Ignatov et al., 2019 – *Ignatov, I., Mehandjiev, D., Vassileva, P., Voykova, D., Karadzhov, S., Gluhchev, G., Ivanov, N.* (2019) Research of Water Catholyte of Presence of Nascent (Atomic) Hydrogen (H*). Hydrogen and Nascent Hydrogen of the Reactions for Origin of Life in Hot Mineral Water. *European Journal of Medicine*. 7(2): 99-105.

Ignatov, 2019 – *Ignatov, I.* (2019). Origin of Life in Hot Mineral Water from Hydrothermal Springs and Ponds. Effects of Hydrogen and Nascent Hydrogen. Analyses with Spectral Methods, pH and ORP. *European Reviews of Chemical Research*. 6(2): 49-60.

Ignatov et al., 2020 – *Ignatov, I., Gluhchev, G., Karadzhov, G., Yaneva, I., Valcheva, N., Dinkov, G., Popova, T., Petrova, T., Mehandjiev, D., Akszjonovich, I.* (2020). Dynamic Nano Clusters of Water on Waters Catholyte and Anolyte: Electrolysis with Nano Membranes. *Physical Science International Journal*. 24(1): 46-54.

Kurihara et al., 2011 – *Kurihara, K., Tamura, M., Shohda, K.* (2011). Self-Reproduction of supramolecular giant vesicles combined with the amplification of encapsulated DNA. *Nature Chemistry*. 4(10): 775-781.

Linsky, 2007 – *Linsky, J.L.* (2007). D/H and Nearby Interstellar Cloud Structures /*Ed. J.I. Linsky. Space Science Reviews, NY*: *Springer Science, Business Media*. 130: 1-367.

Mathews, Moser, 1968 – *Mathews, C.N., Moser, R.* (1968). Peptide Synthesis from Hydrogen-cyanide and Water. *Nature*. 215: 1230-1234.

Miller, 1953 – *Miller, S.L.* (1953). A Production of Amino Acids Under Possible Primitive Earth Conditions. *Science*. 117(3046): 528-529.

Mosin, Ignatov, 2015 – *Mosin, O.V., Ignatov, I.* (2015). Heavy Water as Medium for the Life of Organisms. *Journal of Health, Medicine and Nursing*. 9: 72-110.

Mulkidjanian, Galperin, 2009 – *Mulkidjanian, A.Y., Galperin, M.Y.* (2009). On the Origin of Life in the Zinc World. Validation of the Hypothesis on the Photosynthesizing Zinc Sulfide Edifices as Cradles of Life on Earth.*Biology Direct*. 4: 26-28.

Nakashima, 1987 – *Nakashima, T.* (1987). Metabolism of Proteinoid Microspheres. Ed. T. Nakashima. *Origins of Life and Evolution of Biospheres*. 20(3–4): 269-277.

Nikolis, Prigozhin, 1979 – *Nikolis, P., Prigozhin, I.* (1979). Self-Organization in Non-equilibrium Systems. *Moscow: Mir*. 1-512.

Pons et al., 2011 – *Pons, M.L., Quitte G.., Fujii, T. et al.* (2011). Early Archean Serpentine mud Volcanoes at Isua, Greenland, as a Niche for Early Life. *Proc. Natl. Acad. Sci. U.S.*, 108: 17639-17643.

Schirber, 2010 – *Schirber, M.* (2010). First Fossil-makers in Hot water, *Astrobiology magazine*.

Sugawara, 2011 – *Sugawara, T.* (2011). Self-reproduction of Supramolecular Giant Vesicles Combined with the Amplification of Encapsulated DNA. *Nature Chemistry*. 1127: 775-780.

Szostak, 2011 – *Szostak, J.W.* (2011). An Optimal Degree of Physical and Chemical Heterogeneity for the Origin of Life? *Philos. Trans. Royal Soc. Lond. Biol. Sci.* 366(1580): 2894-901.

Trevors, Pollack, 2005 – *Trevors, J.I., Pollack, G.H.* (2005). Hypothesis: Origin of life in Hydrogel Environment. *Progress in Biophysics and Molecular Biology*. 89(1): 1-8.

Vassileva et al., 2019 – *Vassileva, P., Voykova, D., Ignatov, I., Karadzhov, S., Gluhchev, S., Ivanov, N., Mehandjiev, D.* (2019). Results from the Research of Water Catholyte with Nascent (Atomic) Hydrogen. *Journal of Medicine, Physiology and Biophysics*. 52: 7-11.

# Development the Algorithm for Virtual Screening of Protein Polymorphisms Affecting Their Structural and Functional Properties

Pavel A. Krylov [a], Elena O. Gerasimova [a], Yulia A. Shatyr [a], Alexander B. Mulik [b], Valery V. Novochadov [a], [*]

[a] Volgograd State University, Russian Federation
[b] Federal State-Financed Institution Golikov Research Clinical Center of Toxicology under the Federal Medical Biological Agency, Russian Federation

**Abstract**

The algorithm has been developed for virtual screening of protein polymorphisms that perform various biological functions, primarily related to the regulation of mechanisms at various levels of organization: systemic, cellular, and molecular. The algorithm was developed using the Python v. 3.6.5 programming language in the PyCharm environment. The algorithm includes an automatic search for articles and displays a list that mentions a protein or polymorphism involved in a particular process for specified keywords in PubMed Central. The identified protein and its information are then used to work with the dbSNP database. The algorithm allows sorting polymorphisms according to the following key criteria: whether this polymorphism has been studied or not, whether there is information about its clinical manifestations, the localization of the polymorphism, and the frequency occurrence. The algorithm was tested on the analysis of polymorphisms of the ACAN gene, previously found by automatic search, by keywords characteristic of the functional features of this gene.

As a result, the developed algorithm for virtual screening allowed us to identify polymorphisms of the ACAN gene, according to the stated selection criteria: the total number of polymorphisms (130), their localization in structural and functional domains and in coding (85) or non-coding (52) regions of the gene, as well as the presence of clinical manifestations (136). In the future, the optimization of the algorithm will allow us to obtain more detailed information about certain protein polymorphisms, which will allow us to solve problems in biomedicine, pharmaceuticals, and other biotechnological industries.

**Keywords:** virtual screening, polymorphisms, data bases, PMC, SNP, chondrocytes, ACAN.

## 1. Introduction

At present, heightened interest is directed to the study of the effect of gene polymorphisms on the structural and functional properties of the protein, and subsequently to the identification of their links with the development of diseases. Study of the etiology of such diseases as osteoarthritis (Mori et al., 2014), osteoarthritis (Mikhaylenko et al., 2020), various diseases of the cardiovascular system (Gorący et al., 2020), oncology (Krajewski et al., 2020), psychological diseases (Tretiakov et al., 2020) led to the need to search for and identify gene polymorphisms, as this would make it possible to find out the causes of the development of diseases, and subsequently to select the means for their treatment.

---

[*] Corresponding author
E-mail addresses: novochadov.valeriy@volsu.ru (V.V. Novochadov)

The search and analysis of polymorphisms can be divided into two approaches. The first approach involves the experimental production of mDNA or mRNA, their sequencing and assembly of the genome (genes), followed by decoding and entering the results into the dbSNP database (Mori et al., 2014). The second approach is bioinformatic, which is an automated virtual screening of SNP databases and the identification of those polymorphisms that have not been studied or could be of interest for study for solving problems in various fields of science. In this regard, we chose the second approach, since there is a lot of data on polymorphisms and their number is constantly increasing, and manual analysis requires a lot of time. The lack of programs and algorithms for virtual SNP screening significantly complicates the work with the analysis of polymorphisms.

We set the goal of the work – to develop a virtual screening algorithm, which includes the search for possible proteins, whose polymorphisms are meaningful for study, as well as sorting SNPs according to various criteria.

To test the algorithm, we selected the ACAN gene. Aggrecan protein is expressed from this gene, which provides the structural properties of the cartilage matrix, and also affects the metabolism of chondrocytes (Grogan et al., 2014; Jiang et al., 2018; Satin et al., 2019, Antunes et al. 2020).

**2. Material and methods**
**Libraries and modules used in the work**
The algorithm was developed in the form of a script written in the Python v. 3.6.5 (Python Software Foundation, USA) in PyCharm environment (USA). To develop the algorithm, the following plug-in libraries and modules were used: the Requests v.2.24.0 library was used to implement the request; for searching and selecting information from database sites – library Beautifulsoup4 v.4.9.1 (Plotnikov et al., 2020). The script was executed on the command line, and saved to a Microsoft Excel spreadsheet (Microsoft, USA). As sources of information for the subsequent execution of the algorithm was used the PubMedCentral (National Institutes of Health's National Library of Medicine, USA) and dbSNP (National Center for Biotechnology Information, USA).

**Algorithm stages**
The work was carried out in stages. To visualize the algorithm, a service for the development of interfaces was used – Figma (Figma Inc., USA), Figure 1.

At the first stage, a search query was formed into the PubMedCentral database (gene proliferation AND chondrocyte AND hyaluronan acid), articles should be released in the last ten years. The output of the necessary information includes the title of the article, link and keywords. After the formation of the request and the output of data, the proteins mentioned in the articles were selected.
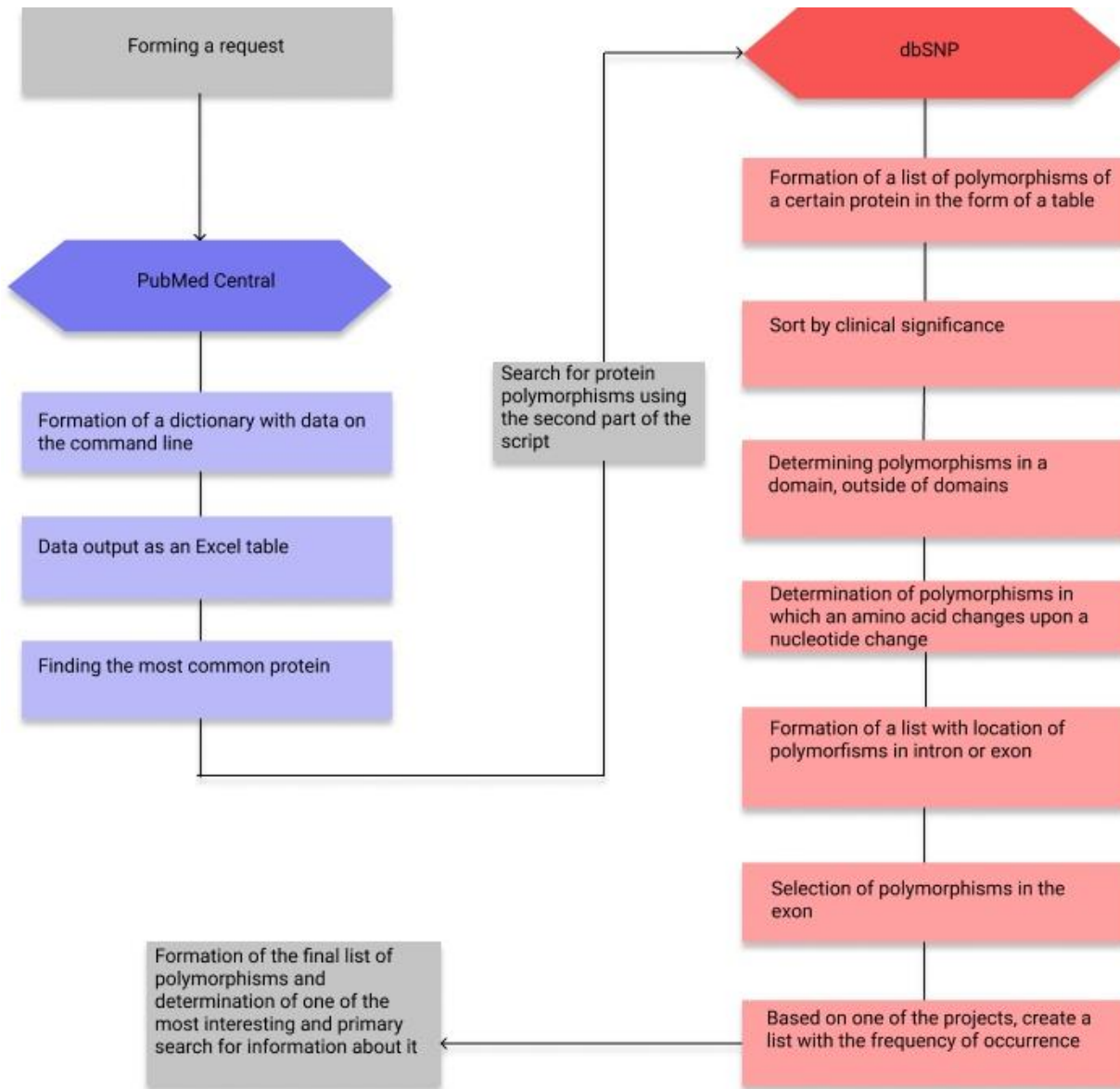
**Fig. 1.** Algorithm block diagram. Intermediate steps without scripts (gray), using the first part of the script to work with PubMedCentral (blue), using the second part of the script to work with dbSNP (red)

The second stage involves working with dbSNP. One protein was selected from the ones found, which is most often mentioned, and through part of the script, the database was parsed and the polymorphisms were sorted. Those polymorphisms were deduced that have clinical manifestations, they are of greater interest. The locations in the domains, intron or exon, and the frequency of occurrence were indicated. To determine the frequency of occurrence, the research of the «1000 Genomes», project was used, the goal of which was to sequence the genomes of approximately 2500 people in the studied populations to create a detailed catalog of human genetic variations. Then polymorphisms that are in the intron and have an average frequency of occurrence are automatically selected.

### 3. Results

As a result of the first part of the script, forty-four articles were found. There are twenty-three articles that mention proteins, the most common protein is Aggrecan (thirteen times). One of the articles, as an example, is shown in Table 1.

**Table 1.** Article title, PubMedCentral link, and referenced proteins

| Article | Link | Proteins |
|---|---|---|
| Effect of Combined Leukocyte-Poor Platelet-Rich Plasma and Hyaluronic Acid on Bone Marrow-Derived Mesenchymal Stem Cell and Chondrocyte Metabolism | https://pubmed.ncbi.nlm.nih.gov/31282189/ | Aggrecan, MMP-9,MMP-13. |

After the execution of the second part of the script, there were definitely one hundred thirty-six polymorphisms with clinical manifestations, then these polymorphisms will be used in the work. An example of several of the polymorphisms is shown in Table 2.

**Table 2.** Clinical manifestation of polymorphism in gene ACAN

| SNP ID | Clinical significance | Name gene |
|---|---|---|
| 1568116 | benign | ACAN |
| 2882676 | benign | ACAN |
| 34124958 | uncertain-significance | ACAN |

Then a list of polymorphisms was formed, determining whether they are in structural or functional domains. The page with information about each polymorphism lists the coding amino acid, its number and whether the amino acid is replaced if the nucleotide changes. To determine the domain, you need the amino acid number. It is based on the complete sequence of the Aggrecan protein (Figure 2) and the nucleotide numbers that are in the domains.
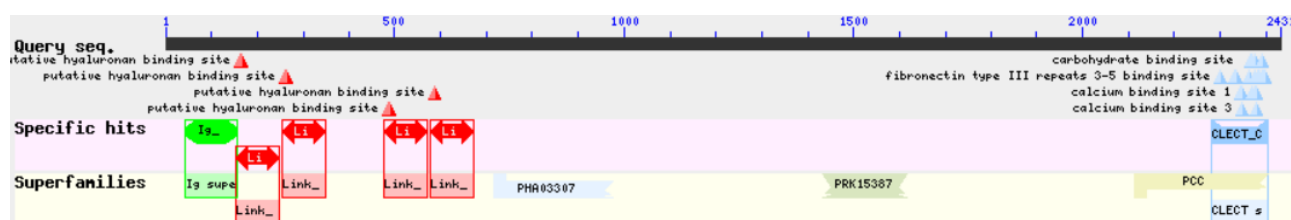


**Fig. 2.** The nucleotide sequence of the Aggrecan protein with domains

Using this sequence, it is possible to determine the boundaries of the domains, that is, from which nucleotide on which structural or functional domains are located. If the nucleotide number of a particular polymorphism is included in any of the boundaries, the output will be "YES", but if the number is not included in the boundaries, then a dash is displayed. An example of a list is shown in Table 3.

**Table 3.** Localization of polymorphism in the functional domain

| SNP ID | Clinical significance | Name gene | Domian |
|---|---|---|---|
| 1568116 | benign | ACAN | YES |
| 2882676 | benign | ACAN | YES |
| 34124958 | uncertain-significance | ACAN | - |

There are 85 in the domains, and 52 polymorphisms outside the domains. Next, you should form a column with the replacement of nucleotides. The data can also be taken from the pages with information about nucleotides. An example of a list in Table 4.

**Table 4.** Information about the replacement of nucleotides in the gene ACAN

| SNP ID | Clinical significance | Name gene | Domian | Replacement |
|---|---|---|---|---|
| 1568116 | benign | ACAN | YES | |
| 2882676 | benign | ACAN | YES | E (Glu) > A (Ala) |
| 34124958 | uncertain-significance | ACAN | - | G (Gly) > D (Asp) |

Next, the SNP in the intron or exon is determined. Information is taken from pages with data on polymorphism, if there is no data on nucleotides (N/A), then "Intron" is displayed in the column, if information is present, then "Exon" is displayed. An example of some polymorphisms is shown in Table 5.

**Table 5.** Localization of the gene ACAN polymorphism in the encoded or non-encoded region mDNA

| SNP_ID | Clinical significance | Name gene | Domian | Replacement | Intron/Exon |
|---|---|---|---|---|---|
| **182894280** | uncertain-significance | ACAN | YES | A (Ala) > T (Thr) | Exon |
| **185836629** | benign | ACAN | - | - | Intron |
| **185960535** | benign | ACAN | - | - | Exon |

Of the specific polymorphisms in the intron, there are six polymorphisms; they are removed from the mRNA by splicing, and therefore are not of particular interest. In the regions that make up the mRNA, that is, in the exons there are 130 polymorphisms.

Further, the frequency of occurrence is determined for these 130 polymorphisms, as it was indicated that for all polymorphisms, data from the 1000 Genomes project are taken. An example of some polymorphisms is shown in Table 6.

**Table 6.** Frequency of occurrence of gene polymorphisms ACAN

| SNP_ID | Clinical significance | Name gene | Domian | Replacement | Intron/Exon | Frequency |
|---|---|---|---|---|---|---|
| **1568116** | benign | ACAN | YES | | Exon | 0,004393 / 22 |
| **2882676** | benign | ACAN | YES | E (Glu) > A (Ala) | Exon | 0,424121 / 2124 |
| **34124958** | uncertain-significance | ACAN | - | G (Gly) > D (Asp) | Exon | 0,027556 / 138 |

Polymorphisms for which data are absent in known sources and data for which are absent are not required. A total of 87 polymorphisms were found. Now one of the polymorphisms has been selected – rs34124958 (Figure 3).



**Fig. 3.** Genomic regions and transcripts gene ACAN

Polymorphism is outside the domains, amino acid substitution occurs, the frequency of occurrence is 0.27556 per 138 people, is of uncertain clinical significance, although it is associated with spondyloepimetaphyseal dysplasia. This disease is a new form of skeletal dysplasia with manifestations of noticeably short stature, facial dysmorphism and characteristic radiographic findings.

## 4. Discussion

To date, three cases have been described, all from the same family. The disease results from a missense mutation affecting the aggrecan C-type lectin domain (AGC1 gene; chromosome 15), which regulates endochondral ossification. Transmission is autosomal recessive (Fukuhara et al. 2019). Most likely, this polymorphism is classified as undefined, since the disease with which it is associated is quite rare and was discovered relatively recently. Since the disease is associated with a domain and amino acid substitution occurs in this polymorphism, it is likely that rs34124958 can change the conformation of the protein in the region with this domain, which leads to disease.

During the development of the algorithm, there were technical difficulties associated with the structure of the SNP database page, but this problem can be eliminated by using additional libraries and scripts. The algorithm can be modified by adding various elements for the accuracy of the search, which can complement existing methods for diagnosing and detecting genetic diseases (Méjécase et al., 2020).

## 5. Conclusion

The developed algorithm is a promising tool for the search for polymorphisms of genes and proteins expressed by them, possessing certain structural and functional properties, and participating in various biological processes. The polymorphism search algorithm can be used to solve a wide range of problems in the field of biotechnology, pharmaceutical industry, and medicine.

## 6. Acknowledgements

## References

Antunes et al., 2020 – *Antunes, B.P., Vainieri, M.L., Alini, M. et al.* (2020). Enhanced chondrogenic phenotype of primary bovine articular chondrocytes in Fibrin-Hyaluronan hydrogel by multi-axial mechanical loading and FGF18. *Acta biomaterialia.* *105*: 170-179. DOI: 10.1016/j.act bio.2020.01.032

Fukuhara et al., 2019 – *Fukuhara, Y., Cho, S. Y., Miyazaki, O. et al.* (2019). The second report on spondyloepimetaphyseal dysplasia, aggrecan type: a milder phenotype than originally reported. *Clinical dysmorphology.* 28(1): 26-29. DOI: 10.1097/MCD.0000000000000241

Gorący et al., 2020 – *Gorący, I., Grudniewicz, S., Safranow, K., et al.* (2020). Genetic polymorphisms of MMP1, MMP9, COL1A1, and COL1A2 in polish patients with thoracic aortopathy. *Disease markers.* 9567239. DOI: 10.1155/2020/9567239

Grogan et al., 2014 – *Grogan, S.P., Chen, X., Sovani, S. et al.* (2014) Influence of cartilage extracellular matrix molecules on cell phenotype and neocartilage formation. *Tissue engineering.* *Part A.* 20(1-2): 264-274. DOI: 10.1089/ten.TEA.2012.0618

Jiang et al., 2018 – *Jiang, X., Liu, J., Liu, Q. et al.* (2018). Therapy for cartilage defects: functional ectopic cartilage constructed by cartilage-simulating collagen, chondroitin sulfate and hyaluronic acid (CCH) hybrid hydrogel with allogeneic chondrocytes. *Biomaterials science.* 6(6): 1616-1626. DOI: 10.1039/c8bm00354h

Krajewski et al., 2020 – *Krajewski, W., Karabon, L., Partyka, A. et al.* (2020) Polymorphisms of genes encoding cytokines predict the risk of high-grade bladder cancer and outcomes of BCG immunotherapy. *Central-European journal of immunology.* 45(1): 37-47. DOI: 10.5114/ceji.2020.94674

Méjécase et al., 2020 – *Méjécase, C., Malka, S., Guan, Z. et al.* (2020). Practical guide to genetic screening for inherited eye diseases. *Therapeutic advances in ophthalmology.* 12: 2515841420954592. DOI: 10.1177/2515841420954592

Mikhaylenko et al., 2020 – *Mikhaylenko, D.S., Nemtsova, M.V., Bure, I.V. et al.* (2020) Genetic polymorphisms associated with sheumatoid arthritis development and antirheumatic therapy response. *International journal of Molecular Sciences*. 21(14): 4911. DOI: 10.3390/ijms 21144911

Mori et al., 2014 – *Mori, Y., Saito, T., Chang, S. H., et al.* (2014). Identification of fibroblast growth factor-18 as a molecule to protect adult articular cartilage by gene expression profiling. *The Journal of biological chemistry*. 289(14): 10192-10200. DOI: 10.1074/jbc.M113.524090

Plotnikov et al., 2020 – *Plotnikov, A., Shcheludyakov, A., Cherdantsev, V. et al.* (2020). Data on post bank customer reviews from web. *Data in brief*. 32: 106152. DOI: 10.1016/j.dib. 2020.106152

Satin et al., 2019 – *Satin, A.M., Norelli, J.B., Sgaglione, N.A., Grande, D.A.* (2019). Effect of combined leukocyte-poor platelet-rich plasma and hyaluronic acid on bone marrow-derived mesenchymal stem cell and chondrocyte metabolism. *Cartilage*. 1947603519858739. DOI: 10.1177/1947603519858739

Tretiakov et al., 2020 – *Tretiakov, A., Malakhova, A., Naumova, E., et al.* (2020). Genetic biomarkers of panic disorder: a systematic review. *Genes*. 11(11): 1310. DOI: 10.3390/genes11111310

# Promising Renewable Raw for Ethanol Biosynthesis

Yuliya A. Zimina [a], Margarita V. Postnova [a], Kais S. Abbas [a],
Kasym S. Abbas [b], Galina S. Ivanova [a], Valery V. Novochadov [a , *]

[a] Volgograd State University, Russian Federation
[b] University of Kirkuk, Iraq

**Abstract**
Ethanol is a valuable product and raw material for various industries, it is widely used as a solvent, fuel, and antiseptic substance. Biotechnology for the production of ethyl alcohol using the microbiological method is rapidly becoming an integral component of global production, as these processes become more efficient and cost-effective. In this regard, an urgent and practically significant direction of research is the development of new technologies and improvement of existing ones to product ethanol based on renewable raw materials. Therefore, it is necessary to systematize the current scientific information in this area. This review examines modern molecular biotechnologies for producing ethanol from various types of renewable raw materials of plant and animal origin. Particular attention we paid to technologies that use waste products from the processing industry, as milk whey, which is a good substrate for ethanol production by the microbiological method. Technologies with the use of various types of microorganisms are considered.
**Keywords:** ethanol, renewable raw materials, alcoholic fermentation, biosynthesis, milk whey, *Saccharomyces cerevisiae*.

## 1. Introduction

Ethanol is widely used in various chemical, fuel, food, perfumery and cosmetic industries. There are two main approaches to product ethanol, using chemical and microbiological methods. According to the first one, we have the so-called industrial alcohol, as a rule, by catalytic hydration of ethylene (Gao et al., 2019).

The reaction is carried out in the presence of high-pressure steam at a temperature of 300 °C, where the ratio of ethylene to steam is 5:3. Catalyst of this reaction is orthophosphoric acid supported on silica gel, activated carbon or asbestos. The reaction scheme is as follows:

$CH_2=CH_2 + H_2O \rightarrow CH_3CH_2OH$.
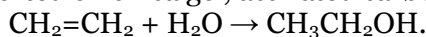
However, hydrocarbon reserves are being depleted and prices for them are steadily growing, therefore, modern technologies are increasingly switching to renewable sources of raw materials, distinguished by their availability and low cost.

Processing plant and animal raw materials led to generation of different organic wastes that require disposal, or secondary products with a lower nutritional value, and therefore having a low cost. Such biomass can be a suitable raw material for microbiological synthesis (biosynthesis) of ethanol for the needs of the medical and food industry. Ethyl alcohol obtained from raw materials of plant or animal origin is also called bioethanol (Busic et al., 2018). It is widely used as a component of fuel mixtures, as well as with a proper degree of purification in medicine and the

---

* Corresponding author
E-mail addresses: novochadov.valeriy@volsu.ru (V.V. Novochadov)

food industry. Thus, the microbiological method for ethanol production is preferable. It allows to use the renewable raw materials, which are waste requiring disposal (Robak et al., 2018; Sarris, Papanikolaou, 2015; Rosales-Calderon, Arantes, 2019).

Ethanol biosynthesis is based on the process of alcoholic fermentation. It may be described as the biological anaerobic converting sugars such as glucose, fructose and sucrose. Microbial enzymes transform sugars into cellular energy without the participation of oxygen, ethanol and carbon dioxide are by-products. In the presence of oxygen, the ethanol biosynthesis is terminated, yeast switches to aerobic respiration, and this phenomenon is called the Pasteur effect (Busic et al., 2018).

Under anaerobic conditions, the rate of glucose metabolism become higher, but the ATP production decreases. When exposed to aerobic conditions, ATP production is increased and the rate of glycolysis slows down. The overall equation for the reaction of alcoholic fermentation is as follows:

$$C_6H_{12}O_6 + 2H_3PO_4 + 2АДФ \rightarrow 2CH_3CH_2OH + 2CO_2 + 2АТФ.$$
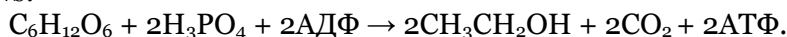
In addition to yeast, such bacteria as *Zymomonas mobilis, Sarcina ventriculi, Erwinia amylovora*, etc. can participate in alcohol fermentation, but bacterial fermentation differs in the amount and nature of by-products. Many studied strains of facultative anaerobic fungi have the same ability. The maximum rate of alcohol formation is characteristic for *Mucoraceae* as *Mucor, Rhizopus,* and *Zygorhynchus*. However, the ethanol yield in these cases is much lower and it is about 5-7 % (Bui et al., 2019; Thanh et al., 2016).

Modern technologies for bioethanol production are represented by two main types: periodic (1) and continuous (2) processes (Robak et al., 2018).

The technologies for producing ethanol using microorganisms differ depending on the feedstock and the specific type of producing organisms. These factors are the main affecting the complexity of the technological scheme, the yield of the target product, and other important indicators to determine the economic efficiency of ethanol production. Next, we will consider the main types of raw materials for ethanol production and the modern technologies corresponding to them.

## 2. Results and discussion
### Starchy raw materials

Root crops as many types of potatoes and grains of corn, barley, and wheat contain a large amount of starch. Starch from various sources can be used for further microbiological conversion to ethanol. Figure 1 shows the structure of starch-containing raw materials used in Russia for ethanol production. As it follows from the diagram, maize accounts for 40 % of all starch-containing raw materials, wheat accounts for 35 %, quarter of all raw materials are rye and other crops (Turshatov et al., 2019).
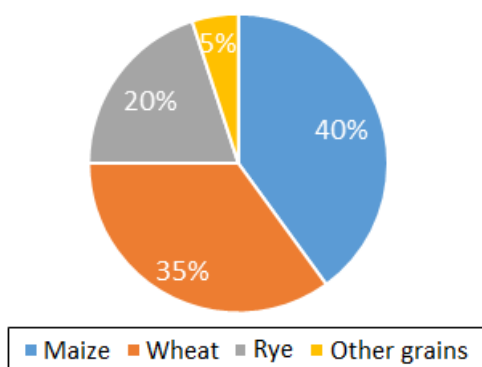


**Fig. 1**. Structure of use of starch-containing raw materials for ethanol production in Russia (data for 2019)

Due to processing raw materials from corn dry and wet methods are useful. Starch-containing raw materials require preliminary hydrolysis with enzyme preparations so that the yeast can convert the substrate into ethanol. Enzymes hydrolyze 1,4- or 1,6- glycoside bonds in amylose and amylopectin, while the first to break the glycoside bonds, using a water molecule as an acceptor. Hydrolysis of starch is carried out under the action of amylolytic enzymes, mainly

α-amylase, β-amylase, and glucoamylase- with the formation of dextrins, oligosaccharides, maltose, or glucose (Mohanty, Swain, 2019; Shahsavarani et al., 2013).

In addition to yeast, there are known methods that use *Bacillus licheniformis* bacteria and genetically modified strains of *Escherichia coli* and *Bacillus subtilis* bacteria that produce α-amylase, as well as mold fungi *Aspergillus niger* and *Rhizopus sp.* producing glucoamylases.

In addition to yeast, methods are known where bacteria *Bacillus licheniformis* and genetically modified strains of bacteria *Escherichia coli* and *Bacillus* subtilis, which produce α-amylase, as well as molds *Aspergillus niger* and *Rhizopus sp.* producing glucoamylases (Busic et al., 2018).

Technologies based on the production of ethyl alcohol from starch are mainly divided into two groups, which differ in the method of boiling down: extrusion processing using pressure (1) and mechanical-enzymatic processing (2).

The first group involves the pretreatment of wheat grains, where coarse grains are mixed with water. The amount of water depends on the starchiness of the grain. After feeding the water emulsion into the the brewer, the batch is subjected to overpressure at an elevated temperature of over 100 ℃. Such harsh conditions, allow to torn the grain shell and destroy the cell structure. Next, the mass is fed into the boil-over. The next stage includes saccharification with the addition of enzyme preparations and subsequent fermentation (Ryabova et al., 2014).

Some of technologies for producing ethanol from wheat use mechanical-enzymatic treatment. For example, the crushed grain is added to water heated to 50 ° C for 30 minutes with preparations containing α-amylase and xylase. The ratio of raw mass and water is 1: 3. The boiling down stage consists of raising temperature to 70 ℃ for 1.5 h, with a subsequent increase to 90 ℃ for 1 hour. After this stage, the process of saccharification of the wort follows with a glucoamylase-containing preparation. The alcohol yield is 65 ml per 100 g of starch. The adding a proteolytic enzyme preparation into saccharified wort increases the alcohol yield to an average of 70 dal/t of starch (Mussatto et al., 2010).

To optimize the enzymatic stage Romaniuk et al. (2015) use especial glucoamylase-containing preparation 'Glucogam' for hydrolysis of wheat at a temperature of 55 ° C. The subsequent fermentation of saccharified mass by the yeast *S. cerevisiae* IMB Y-5007 with feeding diammonium phosphate provided the alcohol yield of 60.7 dal/t of conventional starch. In case of *S. cerevisiae* XII application, the alcohol yield was of 60.6 dal/t of conventional starch.

There are data on the production of ethanol from potato waste using *S. cerevisiae*. A homogeneous suspension consisted of potato flour and water in a ratio of 1:10. The suspension was liquefied with α-amylase at 80 ℃ for 40 min, followed by saccharification with glucoamylase at 65 ℃ for two hours. Fermentation of the hydrolyzate with S. cerevisiae at 35 ℃ for two days resulted in an ethanol yield of 33 g/L (Noufal et al., 2017).

Researchers are also improving methods for producing ethanol using barley. As an example, Bharti B., Chauhan (2016) describe saccharification technology of boiled barley mass with an enzyme preparation of glucoamylase at a temperature of 50−65 ℃ and pH 4.0−5.5 for 120 min. It was found that pH has a multifaceted effect on the saccharification process. On the one hand, hydrogen ions change the ionization of the active center and the conformational state of glucoamylase. On the other hand, they affect the stability of the tertiary structure of glucoamylase. The maximum accumulation of glucose is observed at pH 4.5. The use of multi-enzyme composition results in increasing the glucose amount by 34.7 % compared to the control. The degree of starch hydrolysis increases, since it becomes more accessible for the action of saccharifying enzymes due to the hydrolysis of protein substances and barley grain shells containing hemicelluloses. The use of a multienzyme composition can reduce the consumption of glucoamylase.

The bioconversion of wort prepared on the basis of corn flour into ethanol demonstrates the advantage of extrusion processing in comparison with the traditional mechano-enzymatic method (Peralta-Contreras et al., 2014).

Figure 2 summarizes the process of alcohol production from grain crops.
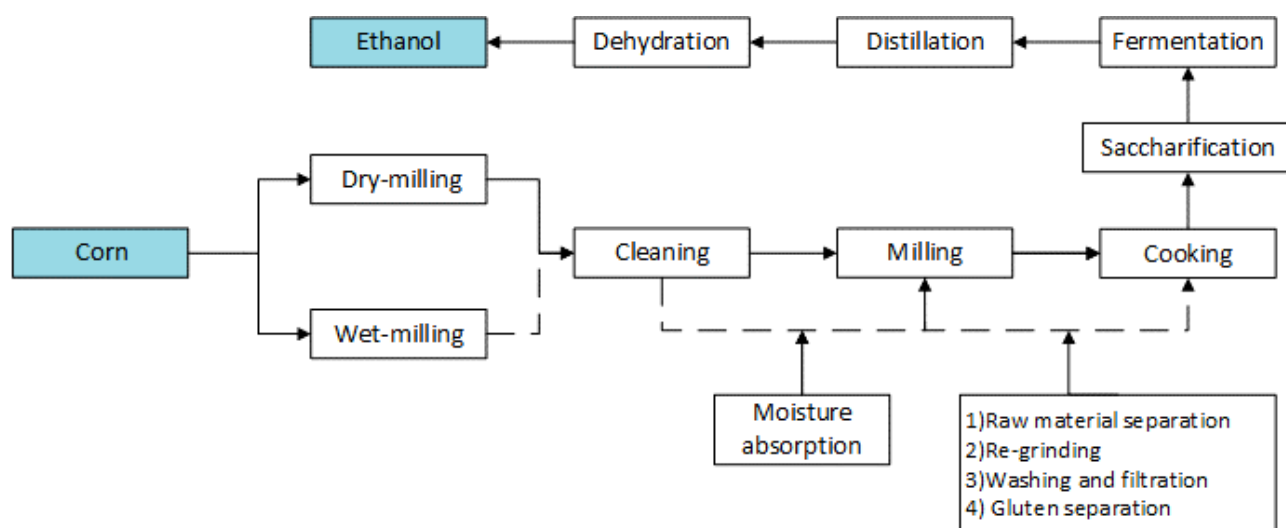
**Fig. 2.** Generalized process of ethanol synthesis of from cereals containing starch

Most of the research is aimed to increase the efficiency of the fermentation through the use of new purified enzyme, microorganisms, and their combinations, as well as by varying the technological parameters of the preliminary feedstock preparation.

**Sugar-containing raw materials**

Sugar cane and beets are the main sources of sugar in the world. Two-thirds of the world's sugar production comes from sugarcane and one third comes from sugar beets. Sugarcane as a raw material for ethanol production has many advantages, as it is a crop that does not require costly agricultural technologies. Sugar cane has a relatively low cost and high reproducibility (Busic et al., 2018). They can be easily hydrolyzed by the β-fructofuranosidase, which is typical enzyme for most *Saccharomyces* species (Reis et al., 2013). Consequently, pretreatment is not required, and this fact makes this process more preferable in comparison to use the starch-contain raw materials. Sugar crops only require a grinding process to extract the sugars into the fermentation medium. Ethanol can also be produced directly from juice or molasses (Eggleston et al., 2010).

In Russia and Europe, sugar production is mainly based on the use of sugar beets as raw materials. The juice formed during the sugar beet processing as an intermediate product, as well as crystalline sugar, can be a raw material for ethanol production. Molasses, being the main by-product of the sugar industry, is widely used in biotechnological industries, including ethanol production. The total residual sugar in molasses can account for 50–60 % of the total mass by volume, the sucrose is about 60 % of this mass, which makes this substrate suitable for large-scale ethanol production (Palmonari et al., 2020). Also, molasses is obtained as a by-product in the drying out citrus pulp with a total sugar content of at least 45 %. The glucose production from starch also produces molasses. Starch molasses contains about 43 % sugars and 73 % solids (Busic et al., 2018).

*S. cerevisiae* are microorganisms that are most often used for the bioethanol production from sugar-containing raw materials. They easily break down sucrose into glucose and fructose. *S. cerevisiae* cells require a small amount of oxygen for the synthesis of fatty acids and sterols during the production of bioethanol; therefore, aeration is an important parameter of this process (Bharti, Chauhan, 2016; Lip et al., 2020). *S. cerevisiae* does not tolerate high concentrations of sugar and salt in the medium and they are also temperature sensitive. Cane molasses medium has the highest osmolarity due to moderate sugar and salt concentrations, which negatively affects ethanol synthesis (Sarris, Papanikolaou, 2015).

Many studies have looked for *S. cerevisiae* strains with higher resistance to salt and temperature (Tekarslan-Sahin et al., 2018; Subodinee et al., 2019; Lip et al., 2020). *Schizosaccharomyces pombe* yeast is also used for bioethanol production as it withstands high salt concentrations and high solids content. In the production of bioethanol, the possibility of using other microorganisms, such as *Zymomonas mobilis, Klebsiella oxytoca, E. coli, Thermoanaerobacter ethanolicus, Pichia stipitis, Candida shehatae, Mucor indicus,* was

investigated (Subodinee et al., 2019). However, no adequate alternative to *S. cerevisiae* has yet been found.

Figure 3 shows schematically a generalized process for the synthesis of ethanol from molasses.
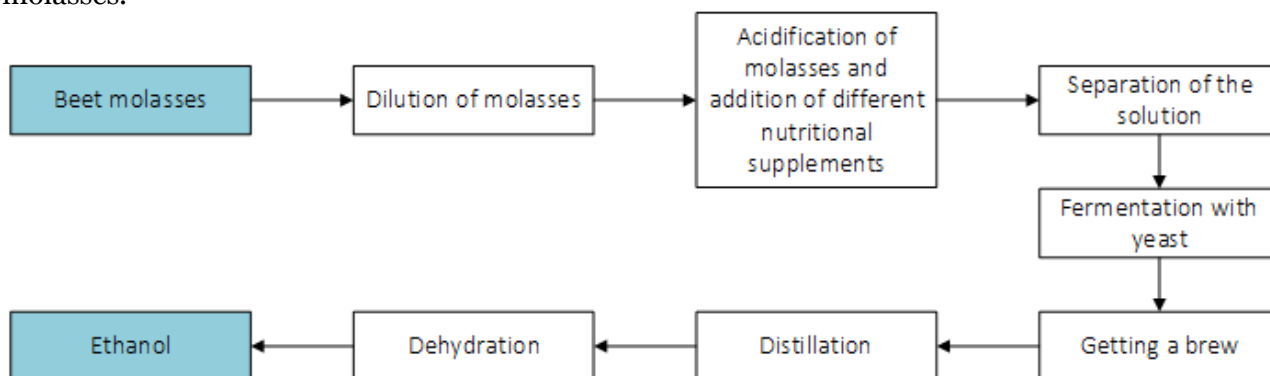


**Fig. 3.** Generalized process for the synthesis of ethanol from molasses

Since the technology for ethanol producing from molasses and other sugar-containing raw materials is simpler in comparison with starch-containing ones, the main research here is aimed at finding exactly new types and strains of microorganisms.

**Lignocellulose-containing raw materials**

The cellulose is surrounded by lignin. In terms of chemical structure, it is a linear β-glucan D-glucose polymer linked by β-1,4-glycosidic bonds. The structure of cellulose is difficult to destroy without enzymatic hydrolysis due to its crystalline nature. The linear cellulose chain consists of 500-14,000 D-glucose units. To transform this rigid crystalline structure from microfibrils in the cell wall into an amorphous structure in water, high temperature and pressure conditions are required at 320 °C and 25 MPa, respectively. These requirements are obviously higher than for starchy raw materials (Subodinee et al., 2019).

Lignocellulosic renewable raw material is promising for ethanol production, since it is also renewable. This raw material can be divided into four groups: plant residues as various cakes, different types of straw and rice husks (1), wood (2), cellulose waste (3), and grass biomass (4). The average lignocellulose mass contains 43 % cellulose, 27 % lignin, 20 % hemicellulose, and 10 % other components (Robak et al., 2018). The diversity of lignocellulosic biomass composition is a disadvantage, since there is a need for more complex and expensive technologies.

The complex structure of lignocellulose requires an additional preliminary stage of raw material preparation. The main problem is that it is necessary to hydrolyze lignocellulose to glucose in order to make it available to microorganisms. Methods of exposure to raw materials include acid and alkaline hydrolysis, enzymatic hydrolysis, transformation under the action of microorganisms, and physico-chemical applications using pressure, steam, radiation, ultrasound, etc. (Amores et al., 2013; Benazzi et al., 2013).

Figure 4 presents a general scheme of this process.
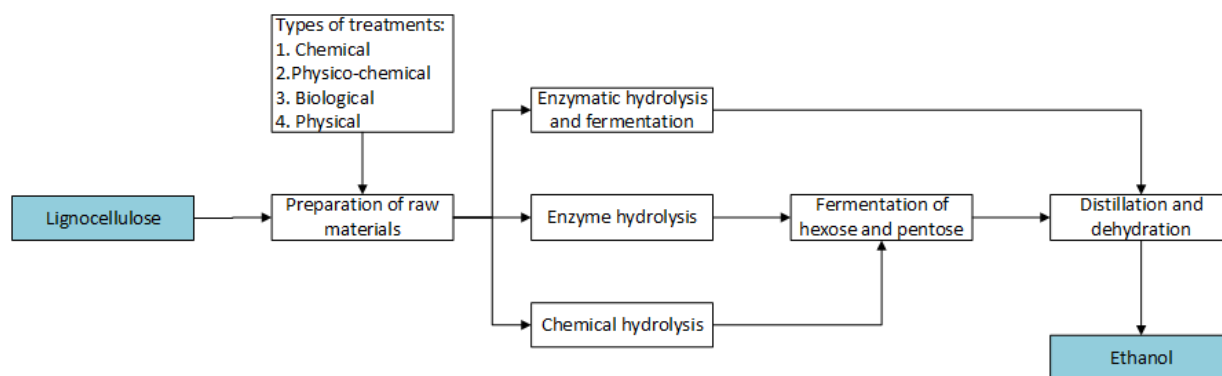


**Fig. 4.** Generalized process for the synthesis of ethanol from lignocellulose

The choice of pretreatment depends on the nature of the feedstock and by-products. This has a great impact on all subsequent stages of ethanol production. Therefore, for the effective use of lignocellulose as a raw material for ethanol production, a careful selection of the preparation stage is required. Further studies of this issue will make it possible to effectively use a large amount of plant waste to obtain a valuable product.

To product the ethyl alcohol, not only vegetable raw materials and also raw materials of animal origin including whey which can be used.

**Milk serum**

Whey being liquid residue after sedimentation and removal of casein from milk during cheese making, contains a large amount of nutrients, about 55 % milk substances. It should be noted that about 9 liters of whey is produced for every 1 kg of cheese. Whey contains lactose of 40 g/L, soluble proteins of 6 g/L, lipids of 4 g/L, vitamins and mineral salts, lactic acid and citric acid, urea and uric acid, β-lactoglobulin, α-lactoglobulin, immunoglobulins, serum albumin and lactoferrin, amino acids, creatine, creatinine, ammonia, etc. Water-soluble vitamins and part of the fat-soluble vitamins of milk as A, B1, B6, C, E, and choline are almost completely transferred to whey. This is a stimulating factor for the development of microorganisms (Dasa et al., 2016).

Whey is the main by-product of the dairy and cheese industry, which is not always or not fully used, therefore it become a liquid waste with a high organic load. The annual production of whey in the world is more than 115 million tons, and according to some estimates, more than 160 million tons, with 47 % ending up in the sewers (Papademas, Kotsaki, 2019). In Russia, according to theoretical calculations, more than 5 million tons per year are produced. At the same time, no more than 30 % of the whey is processed, a small part is used for feeding animals, the rest goes to wastewater (Isina, 2020). In Europe and the USA, more than 80 % of milk whey is used for processing (Pasotti et al., 2017).

Lactose is the main component of whey, which contributes to a high biological oxygen demand (up to 60 g/L) and chemical oxygen demand (up to 80 g/L). If whey enters wastewater, oxygen depletion of water occurs. According to Kieselmann Ru specialists, one ton of whey discharged into a reservoir is, in terms of the damage caused to nature, equal to 100 tons of ordinary household wastewater (Isina, 2020).

In 2019, in the Russian Federation, amendments were made to Federal Law No. 416-FZ of December 7, 2011 'On Water Supply and Wastewater Disposal', which toughen the requirements for the wastewater pollution transferred by factories to water utilities.

Thus, the production of ethanol from whey reduces the need for complex and expensive wastewater treatment processes required for whey disposal. Despite the fact that the conversion of whey to ethanol has proven to be effective in combating liquid waste, the commercialization of ethanol production from whey on an industrial scale is still slow. However, some large-scale whey ethanol production facilities are already operational (Papademas, Kotsaki, 2019; Zabed et al., 2017).

Despite the wide use of various yeast types, attention should be paid to *S. cerevisiae*, since they are actively applied in the alcohol industry, are safe, affordable and the most studied (model) type of microorganisms in biotechnology. One of the most prominent and unique features of these yeasts is their ability to rapidly convert sugars to ethanol both under anaerobic and aerobic conditions. In addition, they are able to withstand a high percentage of medium ethanol compared to other ones (Dong et al., 2015).

The metabolism of *S. cerevisiae* is characterized by the presence of the Crabtree effect known also as catabolic repression, concluding the glucose can partially convert to alcohol despite intense aeration even in an environment with a high sugar concentration. The Crabtree effect is characterized by the simultaneous action of aerobic and anaerobic energy pathways. In this case, the biomass yield varies widely depending on the mass fraction and the nature of the carbohydrate in the medium. It was found for *S. cerevisiae* to suppress synthesis of tricarboxylic acid cycle enzymes, cytochromes and enzymes of the respiratory chain after increasing medium concentration of glucose or fructose more than 0.1 %, even the absence of an oxygen limit. The Crabtree effect is more expressive, when glucose and fructose are used as carbohydrate food, compared with maltose, maltotriose, or galactose application (Robak et al., 2018).

The analysis of modern methods of alcohol obtaining from whey based on lactose fermentation allows to choose four main approaches, which vary depending on the concentration of lactose: the using native unconcentrated whey with a low lactose content (1); the using

concentrated whey with a lactose content of 15–20 % (2); production of alcohol from whey after enzymatic hydrolysis of lactose (3); and the using immobilized microorganisms (4) (Panesar, Kennedy, 2012).

The simplest technologies for the production of ethanol are technologies with application of natural unconcentrated whey. However, it has been found that increasing the lactose concentration in the substrate up to 200 g/L inclusive improves the efficiency of the fermentation (Dasa et al., 2016).

Zohri et al. (2014) carried out a comparative study of natural cheese whey containing 50 g/L of lactose and whey with preliminary deproteinization and concentration of lactose up to 140 g/L. Two strains of *Kluyveromyces marxianus* and four strains of *S. cerevisiae* were studied. Also, authors studied the effect of different initial pH values and addition of four different nitrogen sources to whey. All yeast strains studied were found to be capable of growing and producing ethanol from both original and treated whey. Ethanol production levels range from 3.4 to 18.5 g/L in case of original whey use and from 24.1 to 57.7 g/L when treated whey was applied. Optimum starting pH was 5.5 and yeast extract was the best added nitrogen source. The maximum ethanol levels produced by *K. marxianus* ZMS3GU133329 and *S. cerevisiae* EC1118 from treated whey adjusted to pH 5.5 and supplemented with 0.3 % yeast extract reached 69.9 and 65.4 g/L, which corresponds to 97.8 and 91.4 % of theoretical values, respectively.

The combined use of yeast and lactose-fermenting bacteria is the most effective way of alcohol production, since these microorganisms alone cannot ferment whey without prior hydrolysis. This method does not imply additional power supplies. The presence of lactic acid bacteria in fermentation primarily promotes the hydrolysis of lactose to glucose and galactose. The same time organic acids are produced that can promote the formation of aromatic compounds and lower pH, inhibiting the growth of harmful microorganisms. The adding lactic acid bacteria in the amount of 1 % does not inhibit the growth of yeast. When whey proteins are precipitated using high temperatures, the yield of yeast biomass increases. Heat treatment of whey changes the biological value of the medium. Partial hydrolysis of lactose and whey proteins occurs with the release of more easily digestible half-life products. Therefore, the environment becomes more favorable for yeast growth (Vikhareva et al., 2019).

Figure 5 shows producing ethanol from cheese whey as a generalized diagram.
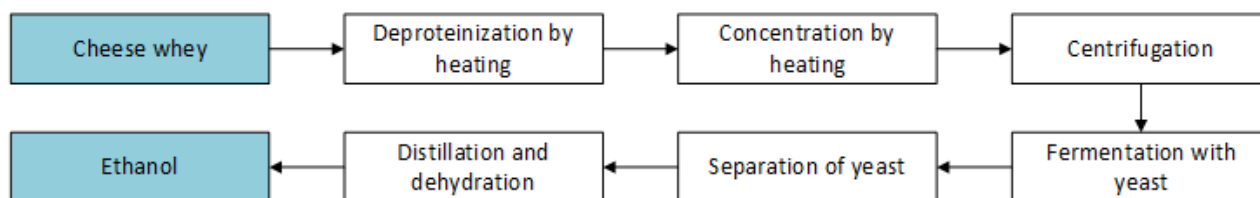


**Fig. 5.** Generalized process of ethanol synthesis from cheese whey

Recent developments in this area are aimed at finding new microorganisms capable of efficiently fermenting sugars with the formation of ethanol.

Japanese scientists discovered the ability of the brown rot fungi *Neolentinus lepideus* to ferment lactose into ethanol. The ability of the fungus to ferment lactose is not affected by the addition of glucose or calcium, as is the case with yeast. The fermentation is effective at pH = 2–3 and temperature 28 °C; the fermentation time is 48 hours. The process occurs regardless of the whey concentration, but it needs to be deproteinized. Therefore, *N. lepideus* may be useful in the ethanol production from materials consisting mainly of lactose, such as cheese whey or expired cow's milk (Okamoto et al., 2019).

Whey permeate is the lactose-rich liquid remaining after protein extraction from cheese whey. Artificially created microorganisms specially designed for fermentation of milk waste have been proposed for this technology. Eight *E. coli* strains were metabolically constructed using a new expression plasmid with genes of enzymes converting pyruvate to ethanol. The best strain among the candidates was selected according high ethanol yield. It has been shown for this constructed microorganism to be capable of efficiently fermenting whey permeate without food additives. The selected strain of *E. coli* lends itself to further optimization of metabolism and, according to

the authors opinion, represents a step forward in the direction of efficient production of bioethanol from industrial waste (Pasotti et al., 2017).

Since *S. cerevisiae* yeast does not have a lactose metabolism system, modern research is aimed at finding ways to improve their strains. To construct lactose-consuming *S. cerevisiae* strains, approaches involving the expression of lactose genes of the phylogenetically related yeast *Kluyveromyces lactis*, as well as lactose genes from *E. coli* and *A. niger*, were used (Domingues et al., 2010).

Various bioengineering strategies have been applied including the use of genes for lactose metabolism from bacteria *E. coli*, yeast *K. lactis*, and *A. niger*. In study the metabolic engineering of *S. cerevisiae* cells for converting lactose to ethanol, the best results were obtained with recombinants engineered with *K. lactis* genes. Nevertheless, direct cloning of LAC4 and LAC12 from *K. lactis* with its own promoter did not allow direct selection of transformants in samples with lactose and led to recombinants with a slow growth phenotype (Malakar et al., 2020). Thus, we can conclude that this method is laborious and unstable.

## 3. Conclusion

The microbiological method for ethanol producing is promising both from the point of view of its increasing efficiency, and from the point of view of utilizing waste of plant and animal origin. Technologies differ depending on the feedstock and the specific type of producing organisms. The most promising raw material is milk whey, since its processing into alcohol is of particular environmental importance allowing to reduce the amount of wastewater and pollution of natural water reservoirs.

The search for new types and strains of microorganisms with low pathogenicity, resistant to harsh environmental conditions, allowing the process to be carried out with a maximal alcohol yield is the main scientific direction in this field. Here the most promising are further studies using bioinformatics methods and various bioengineering approaches.

## References

Amores et al., 2013 – *Amores I., Ballesteros I., Manzanares P. et al.* (2013). Ethanol production from sugarcane bagasse pretreated by steam explosion. *Electron J. Energy Environ.* 1(1): 25-36. DOI: 10.7770/ejee-V1N1-art519

Benazziet al., 2013 – *Benazzi, T., Calgaroto, S., Astolfi, V. et al.* (2013). Pretreatment of sugarcane bagasse using supercritical carbon dioxide combined with ultrasound to improve the enzymatic hydrolysis. *Enzyme Microb. Technol.* 52(4-5): 247-250. DOI: 10.1016/j.enzmictec. 2013.02.001

Bharti, Chauhan, 2016 – *Bharti, B., Chauhan, M.* (2016). Bioethanol production using Saccharomyces cerevisiae with different perspectives: substrates, growth variables, inhibitor reduction and immobilization. *Ferment. Technol.* 5(2): e1000131. DOI: 10.4172/2167-7972.1000131

Bui et al., 2019 – *Bui, L.T., Novi, G., Lombardi, L. et al.* (2019). Conservation of ethanol fermentation and its regulation in land plants. *J. Exp. Bot.* 70(6): 1815-1827. DOI: 10.1093/jxb/erz052

Busic et al., 2018 – *Busic, A., Mardetko, N., Kundas, S., et al.* (2018) Bioethanol production from renewable raw materials and its separation and purification: areview. *FoodTechnol. Biotechnol.* 56(3): 289-311. DOI: 10.17113/ftb.56.03.18.5546

Dasa et al., 2016 – *Dasa, M., Raychaudhurib, A., Ghosh, S.K.* (2016). Supply chain of bioethanol production from whey: a review. *Proc. Environ. Sci.* 35: 833-846. DOI: 10.1016/ j.proenv.2016.07.100

Domingues et al., 2010 – *Domingues, L., Guimaraes, P.M.R., Oliveira, C.* (2010). Metabolic engineering of Saccharomyces cerevisiae for lactose/whey fermentation. *Bioengineered Bugs.* 1(3): 164-171. DOI: 10.4161/bbug.1.3.10619

Dong et al., 2015 – *Dong, S.-J., Yi, C.-F., Li, H.* (2015). Changes of Saccharomyces cerevisiae cell membrane components and promotion to ethanol tolerance during the bioethanol fermentation. *Int. J. Biochem. Cell Biol.* 69: 196-203. DOI: 10.1016/j.biocel.2015.10.025

Eggleston et al., 2010 – *Eggleston, G., Tew, T., Panella, L., Klasson, K.* (2010). Ethanol from sugar crops. *Industr. Crops Uses.* 60-83. DOI: 10.1079/9781845936167.0060.

Gao et al., 2019 – *Gao, J., Li, Z., Dong, M. et al.* (2019). Thermodynamic analysis of ethanol synthesis from hydration of ethylene coupled with a sequential reaction. *Front. Chem. Sci. Eng.* 14: 847-856. DOI: 10.1007/s11705-019-1848-6

Isina, 2020 – *Isina, N.Y.* (2020). Financial mechanism for the implementation of environmentally oriented technology of milk whey processing. *Proc. Kostroma State Agricultural Academy.* 90: 111-119.

Lip et al., 2020 – *Lip, K.Y.F., García-Ríos, E., Costa, C.E. et al.* (2020). Selection and subsequent physiological characterization of industrial Saccharomyces cerevisiae strains during continuous growth at sub- and- supra optimal temperatures. *Biotechnol. Rep. (Amst).* 26: e00462. DOI: 10.1016/j.btre.2020.e00462

Malakar et al., 2020 – *Malakar, S., Paul, S.K., Pou, K.R.J.* (2020). Biotechnological interventions in beverage production. *Biotechnol. Progr. Beverage Consump.* 19: 1-37. DOI: 10.1016/B978-0-12-816678-9.00001-1

Mohanty, Swain, 2019 – *Mohanty, S.K., Swain, M.R.* (2019). Chapter 3 – Bioethanol production from corn and wheat: food, fuel, and future. In: Bioethanol Production from Food Crops. Sustainable Sources, Interventions, and Challenges. *Academic Press*: 45-59.

Mussatto et al., 2010 – *Mussatto, S.I., Dragone, G., Guimarães, P.M.R. et al.* (2010). Technological trends, global market, and challenges of bio-ethanol production. *Biotechnol. Adv.* 28(6): 817-830.

Noufal et al., 2017 – *Noufal, M., Li, B., Maalla, Z.* (2017). Production of bio ethanol from waste potatoes. *IOP Conference Series: Earth Environ. Sci.* 59: e012006. DOI: 10.1088/1755-1315/59/1/012006

Okamoto et al., 2019 – *Okamoto, K., Nakagawa, S., Kanawaku, R.* (2019). Ethanol production from cheese whey and expired milk by the brown rot fungus Neolentinus lepideus. *Fermentation.*5(2): e49. DOI: 10.3390/fermentation5020049

Palmonari et al., 2020 – *Palmonari, A., Cavallini, D., Sniffen, C.J. et al.* (2020). Short communication: Characterization of molasses chemical composition. *J. Dairy Sci.* 103(7):6244-6249. DOI: 10.3168/jds.2019-17644

Panesar, Kennedy, 2012 – *Panesar, P.S., Kennedy, J.F.* (2012). Biotechnological approaches for the value addition of whey. *Crit. Rev. Biotechnol.* 32(4): 327-348. DOI: 10.3109/07388551.2011.640624

Papademas, Kotsaki, 2019 – *Papademas, P., Kotsaki, P.* (2019). Technological utilization of whey towards sustainable exploitation. *Adv. Dairy Res.* 7: e231. DOI: 10.35248/2329-888X.19.7.23

Pasotti et al., 2017 – *Pasotti, L., Zucca, S., Casanova, M., et al.* (2017) Fermentation of lactose to ethanol in cheese whey permeate and concentrated permeate by engineered Escherichia coli. *BMC Biotechnology.* 17(1): e48. DOI: 10.1186/s12896-017-0369-y

Peralta-Contreras et al., 2014 – *Peralta-Contreras, M., Aguilar-Zamarripa, E., Pérez-Carrillo, E. et al.* (2014). Ethanol production from extruded thermoplastic maize meal by high gravity fermentation with Zymomonas mobilis. *Biotechnol. Res. Int.* e654853. DOI: 10.1155/2014/654853

Reis et al., 2013 – *Reis, V.R., Bassi, A.P., Silva, J., Antonini, S.* (2013). Characteristics of Saccharomyces cerevisiae yeasts exhibiting rough colonies and pseudohyphal morphology with respect to alcoholic fermentation. *Braz. J. Microbiol.* 44(4): 1121-1131. DOI: 10.1590/S1517-83822014005000020

Robak et al., 2018 – *Robak, K., Balcerek, M.* (2018). Review of second generation bioethanol production from residual biomass. *Food Technol. Biotechnol.* 56(2): 174-187. DOI: 10.17113/ftb.56.02.18.5428

Romaniuk et al., 2015 – *Romaniuk, T.I., Agafonov, G.V., Frolova, N.N.* (2015). Development of technology for wheat processing into alcohol and protein product. *J. Voronezh State Univ. Eng. Technol.* (1): 138-142.

Rosales-Calderon, Arantes, 2019 – *Rosales-Calderon, O., Arantes, V.* (2019). A review on commercial-scale high-value products that can be produced alongside cellulosic ethanol. *Biotechnol Biofuels.* 12: e240. DOI: 10.1186/s13068-019-1529-1

Ryabova et al., 2014 – *Ryabova, S.M., Lazareva, I.V., Semenenko, N.T.* (2014). Development of high-performance ethanol technology from rye using succinic acid Part II. The stage of wort fermentation. *Beer Beverages Msc.* 5: 32-35.

Sarris, Papanikolaou, 2015 – *Sarris, D., Papanikolaou, S.* (2015). Biotechnological production of ethanol: biochemistry, processes and technologies. *Eng. Life Sci.* 16: 307-329. DOI: 10.1002/elsc.201400199

Shahsavarani et al., 2013 – *Shahsavarani, H., Hasegawa, D., Yokota, D. et al.* (2013). Enhanced bio-ethanol production from cellulosic materials by semi-simultaneous saccharification and fermentation using high temperature resistant Saccharomyces cerevisiae TJ14. *J. Biosci. Bioeng.* 115(1): 20-23.

Subodinee et al., 2019 – *Subodinee, M., Mizutani O., Toyama, H.*(2019). Yeast strains from coconut toddy in Sri Lanka show high tolerance to inhibitors derived from the hydrolysis of lignocellulosic materials. *Biotechnol.Biotechnol. Equip.* 33: 1505-1515. DOI: 10.1080/13102818.2019.1676167.

Tekarslan-Sahin et al., 2018 – *Tekarslan-Sahin, S.H., Alkim, C., Sezgin, T.* (2018). Physiological and transcriptomic analysis of a salt-resistant Saccharomyces cerevisiae mutant obtained by evolutionary engineering. *Bosn. J. Basic Med. Sci.* 18(1): 55-65. DOI: 10.17305/bjbms. 2017.2250

Thanh et al., 2016 – *Thanh, V.N., Thuy, N.T., Chi, N.T. et al.* (2016). New insight into microbial diversity and functions in traditional Vietnamese alcoholic fermentation. *Int. J. Food Microbiol.* 232(1): 15-21. DOI: 10.1016/j.ijfoodmicro.2016.05.024

Turshatov et al., 2019 – *Turshatov, M.V., Krivchenko, V.A., Solov'ev, A.O.* (2019). Analysis of technological factors affecting the qualitative composition of dietary fiber in the processing of grain for alcohol. *Beer Beverages Msc.* 4: 65-68.

Vikhareva et al., 2019 – *Vikhareva, E.A., Khodyashev, N.B.* (2019). About technological aspects of processing lactose of the milk whey. *Chemistry. Ecology. Urbanistics. Perm.* 1: 364-367.

Zabed et al., 2017 – *Zabed H., Sahu J.N., Suely A. et. al.* (2017). Bioethanol production from renewable sources: current perspectives and technological progress. *Renewable Sustainable Energy Rev.* 71(C): 475-501. DOI: 10.1016/j.rser.2016.12.076

Zohri et al., 2014 – *Zohri, A.–N.A., Gomah, N.H., Maysa, A.A.* (2014). Utilization of cheese whey for bio–ethanol production. *Univ. J. Microbiol. Res.* 2(4): 57-73. DOI: 10.13189/ujmr.2014.020401